energies

MDPI

Article

Modelling and Simulation/Optimization of Austria's National Multi-Energy System with a High Degree of Spatial and Temporal Resolution

Matthias Greiml *, Florian Fritz, Josef Steinegger, Theresa Schlömicher, Nicholas Wolf Williams, Negar Zaghi and Thomas Kienberger

Energy Network Technology, Montanuniversitaet of Leoben, 8700 Leoben, Austria
* Correspondence: matthias.greiml@unileoben.ac.at

Abstract: The European Union and the Austrian government have set ambitious plans to expand renewable energy sources and lower carbon dioxide emissions. However, the expansion of volatile renewable energy sources may affect today's energy system. To investigate future challenges in Austria's energy system, a suitable simulation methodology, temporal and spatially resolved generation and consumption data and energy grid depiction, is necessary. In this paper, we introduce a flexible multi-energy simulation framework with optimization capabilities that can be applied to a broad range of use cases. Furthermore, it is shown how a spatially and temporally resolved multi-energy system model can be set up on a national scale. To consider actual infrastructure properties, a detailed energy grid depiction is considered. Three scenarios assess the potential future energy system of Austria, focusing on the power grid, based on the government's renewable energy sources expansion targets in the year 2030. Results show that the overwhelming majority of line overloads accrue in Austria's power distribution grid. Furthermore, the mode of operation of flexible consumer and generation also affects the number of line overloads as well.

Keywords: 100% renewable energy sources (RESs); multi-energy system (MES) modelling; multi-energy system (MES) simulation; hybrid grid; national multi-energy system (MES)

Citation: Greiml, M.; Fritz, F.; Steinegger, J.; Schlömicher, T.; Wolf Williams, N.; Zaghi, N.; Kienberger, T. Modelling and Simulation/Optimization of Austria's National Multi-Energy System with a High Degree of Spatial and Temporal Resolution. *Energies* **2022**, *15*, 3581. https://doi.org/10.3390/en15103581

Academic Editors: Zbigniew Leonowicz, Michał Jasiński and Arsalan Najafi

Received: 20 April 2022
Accepted: 10 May 2022
Published: 13 May 2022

1. Introduction

Climate change is seen as a serious problem by ninety-three per cent of Europeans. According to the European Commission, the same number of Europeans have taken at least one action to tackle climate change. By setting up the ambitious "European Green Deal" program in December 2019, the European Commission aims to achieve a climate-neutral European Union by 2050 [1,2]. Concretizing the path towards achieving "European Green Deal" targets, the European Commission set up the "Fit for 55" program as an interim goal in July 2021. This program aims to reduce the European Union's carbon dioxide emissions by fifty-five per cent by the year 1990 [3].

As a member of the European Union, the Austrian government has set even more ambitious targets, aiming to achieve net CO_2 neutrality by 2040 [4]. Furthermore, the Austrian #mission2030 aims to achieve a hundred per cent renewable power generation net-balanced over one year until the year 2030. To achieve this target, renewable energy sources (RES), mainly volatile wind and photovoltaics, have to be expanded significantly [5].

The enhanced usage of RESs presents challenges for both the energy system and its operators since RESs are decentralized, hardly predictable, and introduce volatility into energy grids [6]. Achieving a hundred per cent RES might require:

- A spatial and timely compensation of energy;
- An increase in flexibility for both demand and generation in an energy system;
- The ability to cope with high instantaneous penetration of RES;

- Curtailment of RES as ultima-ratio.

In order to integrate a high share of RESs into existing energy systems and to avoid previously described issues, new approaches are necessary. In recent years, research focused on a cross-sectoral approach to consider the energy carriers' individual advantages in an energy system. This approach allows for the implementation of power, natural gas, district heating, hydrogen, and carbon dioxide grids, combined with storage and sector coupling (SC) options [7].

A need to address previously described challenges can be derived by looking at the distribution of RES in Austria. Sejkora et al. [8] provide a comprehensive overview of Austria's spatial distribution of technical exergy potentials of RES, which can be directly converted into RES energy potential [8]. Referring to Figure 1, it can be seen that renewable potentials are widely spread all over Austria, fluctuating in both the type of RES and the quantity in each district. However, it can be seen that wind potentials are mainly to be found in eastern Austria, whereas hydropower potentials are located in the western parts of Austria. Biomass and photovoltaics can be considered as more evenly distributed across Austria.

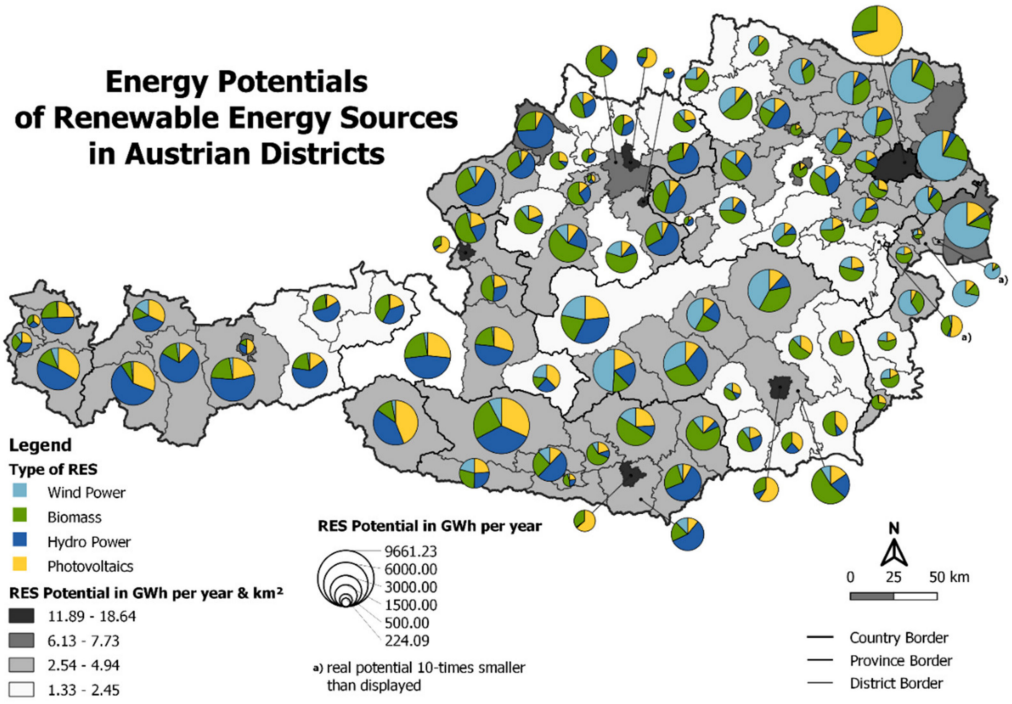

Figure 1. Technical energy potentials of RES per Austrian district, derived from [8,9].

Integrating further RES into the current energy system might lead to issues as previously disclosed. To address them, we introduce an updated multi-energy-system (MES) simulation framework, HyFlow, and discuss simulation results based on potential scenarios of the Austrian energy system in the year 2030.

1.1. Literature Overview and Research Need

As there are numerous publications on the topic of MES models, this section aims to display the current state of research regarding MES simulation and optimization approaches. Furthermore, we introduce research focusing on Austria's national multi-energy system models.

1.1.1. MES Simulation and Optimization Approaches

According to Klemm and Vennemann [10], energy system models can be methodologically categorized in optimization, forecasting/simulation, and back-casting. Depending on

the defined objective function, optimization is capable of determining an optimal solution or scenario. Forecasting or Simulation models show the system's behavior according to the selected input parameter. This scenario-based approach likely doesn't represent an optimal solution with regard to the selected boundary conditions. In back-casting models, an envisioned future state or properties are defined. Based on the future state, the back-casting model develops paths to these future conditions. Further categorization criteria could be assessment criteria, as well as analytical or mathematical approaches and challenges. The structural and technological details of MES models can include geographic coverage, spatial and temporal resolution, time horizon, sectoral coverage, and demand sectors [10].

Several pieces of research provide a comprehensive overview and comparison of existing MES assessment approaches, such as [10–14]. As can be seen in the before-mentioned sources, the predominant modelling approach for MES is optimization followed by simulation. Since the methodology described in this paper can be categorized as an MES simulation model, the following section focuses on MES simulation models. Still, it will also display differences compared to optimization models.

Bottechia et al. [12] introduce the modular, multi-energy carrier, and multi-nodal multi-energy system simulator (MESS). The framework is designed for urban areas; however, wider spatial coverage is also possible. The authors compare and investigate the cause of differences of MESS results with Calliope (MES optimization framework), based on a simple MES. The outcome of both methods tends to be similar yet different due to the individual model's target function and mode of operation. One further advantage of MESS over Calliope is a much faster computation time. A main disadvantage of MESS might be that only one grid level can be depicted [12].

A combination of Pandapower [15] and Pandapipes [13] is proposed by Lohmeier et al. [13] to create a multi-energy grid simulation framework with a focus on detailed energy grid depiction. The so-called multi-energy controller, similar to the energy hub concept, allows for the implementation of sector coupling or energy storage options. The authors demonstrate the capabilities of the MES simulation framework based on two use cases. Since detailed energy grid calculations, as well as multi-energy controllers, are computation time intensive tasks, one disadvantage of the proposed model is extensive computation time, when simulating a full year in 15 min time steps [13].

Böckl et al. [16] introduces a previous version of the MES simulation framework HyFlow, which is utilized for various research questions, such as [17–19]. By applying HyFlow, potential fields of improvements became visible, since the previous HyFlow version is not capable of addressing issues, such as:

- More than two individual network levels;
- No energy transfers across various network levels, since only step-by-step energy transfer via each network level is possible (energy must always flow via each network level without skipping network levels);
- A lack of selectable control strategies for both sector coupling and energy storage options;
- Implementation of further components of an energy system is only possible with high programming effort.

In [20,21], an MES optimization framework is proposed, consisting of individual energy hubs, interconnected with individual energy grids. Both models provide a two-stage optimization for the energy hub and the whole system. In dependence of the target function, individual research questions are addressed.

1.1.2. MES Investigations on National Level

This section aims to provide an overview of existing research on national MESs to demonstrate current research approaches.

Sejkora et al. [22] display how Austria's future energy system could be composed if exergy efficiency is defined as optimization criteria in a fully decarbonized energy system, where RES are expanded according to #mission2030 targets [5,22]. The research shows that

with restricted RES expansion in Austria, significant imports of sustainable methane and hydrogen will be necessary in the future. This research can provide guidelines for future technologies in MES, but cannot address any spatial problems [22]. In comparison, the project ONE100 from Austrian Gas Grid Management shows an energy system where RES are expanded until their maximum potential. In this case, import demand is significantly reduced to four per cent of total energy consumption. This research aims to achieve an economically optimized energy system. The model contains a rough spatial resolution of Austria, dividing Austria into 19 interconnected regions [23].

In [24], a comprehensive overview of research in the field of optimizing national energy system models is provided. However, the spatial resolution of each model shown is quite low. A lack of subnational data availability is seen as the main reason for the low spatial resolution [24].

1.1.3. Research Need

Flexible MES simulation frameworks to cover a wide range of individual problems are not available yet. Furthermore, to the best of our knowledge, it has never been attempted before to set up a national MES simulation model with detailed spatial resolution and detailed infrastructure depiction.

In this paper, we aim to close previously described scientific gaps by presenting a new version of our self-developed MES simulation framework HyFlow and demonstrate its capabilities based on Austria's energy system in 2030. The following research questions are to be investigated in this paper:

- Based on the scientific gap, how should an MES simulation framework be designed to cope with a national MES and various other research questions with a high degree of both spatial and temporal resolution?
- What steps have to be taken to model Austria's national energy system with detailed spatial and temporal resolution?
- What are the effects on power infrastructure based on #mission2030 renewable energy sources expansion, considering different modes of flexibility operation and power load flow optimization?

To answer the research questions this paper is structured as follows. The following subchapter describes considered challenges modelling the Austrian energy system. In Section 2, the methodology to set up an MES simulation framework and national MES model is described. Investigated scenarios and their corresponding results are disclosed in Sections 3 and 4, respectively. Simulation results are discussed in Section 5, followed by a conclusion and an outlook for potential further research in Section 6.

1.2. Problem Description

To address previously mentioned research questions, various obstacles need to be addressed beforehand. As demonstrated in the literature research, MES simulation frameworks that are currently available can be significantly improved to address a wide and flexible range of research questions, especially in the following fields:

- The flexible depiction of various network levels of all energy carriers (power, gas, heat), independent of spatial resolution. This should enable a large range of spatial resolution to be able to depict various areas, from single consumers up to the state level.
- The possibility to assign various flexibility options, such as sector coupling technologies, storage options, demand-side management (DSM), and operation-flexible power plants. This should include the possibility of flexibly adding any further components to expand the MES framework's functionality. Flexibilities may operate, e.g., as load following units or with various optimization-based operation strategies, such as maximizing profits or maximizing the degree of self-sufficiency in a specified area.

- State of art load flow consideration via adequate load flow calculation for all considered energy carriers. Depending on the user's selection, power flow simulation or optimal power flow load flow calculations should be selectable for the power grid.

The updated HyFlow MES simulation framework can address the previously mentioned points to develop a generic and flexible MES simulation framework.

As outlined in [24], a lack of subnational data is a major challenge when modelling a national MES. This challenge is addressed twice in this paper:

- Suitable approaches and data to be found to achieve a detailed spatial resolution. This includes consumption and generation data for all energy carriers. If data are not available in low spatial resolution, a suitable approach must be found to distribute general data towards smaller entities.
- Currently, no models of Austria's power, natural gas, and district heating energy infrastructure are openly available. To allow for the consideration of real grid properties, an energy grid model must be developed, based on available data to depict the Austrian energy infrastructure.

To demonstrate the capabilities of HyFlow, three scenarios of the Austrian energy system in the year 2030 are simulated to show the effects of RES expansion and various modes of operation of flexibilities, such as heat pumps, electric vehicles, power storage, and gas-fired power plants.

2. Methodology

This section is split into two main parts to provide a methodological overview of the HyFlow MES simulation framework and all the necessary steps to create an MES model of Austria, to be assessed with HyFlow.

2.1. HyFlow

To provide a comprehensive overview of the HyFlow MES simulation framework, the general modelling structure, the input data, the calculation procedure, and the implementation of flexibility options are discussed in the following sub-chapters.

2.1.1. General Modelling Structure

In HyFlow, the examined area can be divided into several cells. In this work, so-called substation districts are used (refer to Section 2.2.5. Spatial Data Distribution). This approach is called the cellular approach; further details can be found in [16]. All entities within one cell are aggregated into its corresponding cell. Therefore, a cell represents the smallest spatially resolved area, resulting in a node. In Figure 2, an example of a single node is displayed. To implement consumption and generation in one single term, the term "residual load" (RL) is used and defined as per Equation (1).

$$P_{RL}[t] = P_{demand}[t] - P_{Generation}[t] \quad (1)$$

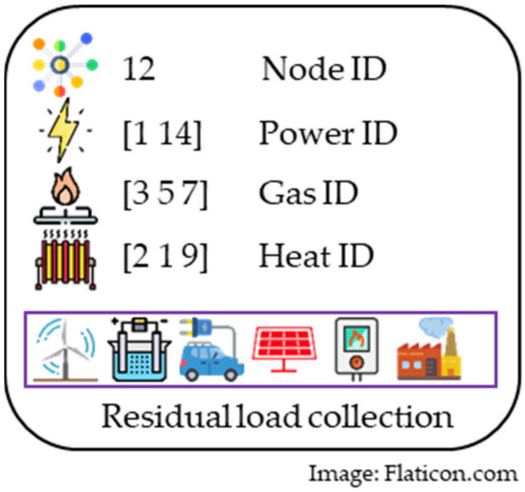

Figure 2. Example of a single node.

In Table 1, an overview of the node parameters is provided. Further parameters such as maximum and minimum voltage, pressure, and temperature can also be defined.

Table 1. Overview node class parameters.

Parameter	Type	Description
Node ID	scalar	One unique number is assigned to each node.
Power ID	1 by 2 vector	Vector at [1 1] is currently a spare parameter. Vector at [1 2] indicates the node's position in the power grid.
Gas ID	1 by 3 vector	Vector at [1 1] indicates the node's pressure level (e.g., 2 = 70 bar). Vector at [1 2] indicates the node's subgroup. Vector at [1 3] indicates the node's number within the subgroup.
Heat ID	1 by 3 vector	Please refer to Gas ID.
RL collection	array	This array contains all objects, and their behavior can be expressed in active and reactive power, gas, or heat RL. Power RL is defined as per Equation (1), valid for all other energy carriers too. The RL collection in Figure 2 includes wind energy, electrolysis, electric car, photovoltaics, gas to heat (GtH), and an industrial consumer.

Nodes can be interconnected with other nodes. Depending on the availability of energy grids, a node-edge depiction is established. An example of several nodes with various connections of energy carriers (edges) is shown in Figure 3. It can be seen that all nodes are connected to the power grid. Nodes 12, 13, 14, and 327 represent one gas sub-grid. Node number 14 supplies gas to a lower pressure network (since the first vector position of gas ID is higher), consisting of nodes 26 and 27. As an example of RL collection objects, further implementable objects that can be added to a node's RL collection, such as consumer, producer, sector coupling technology, storage options, and electric vehicles, are shown adjacent to their corresponding node.

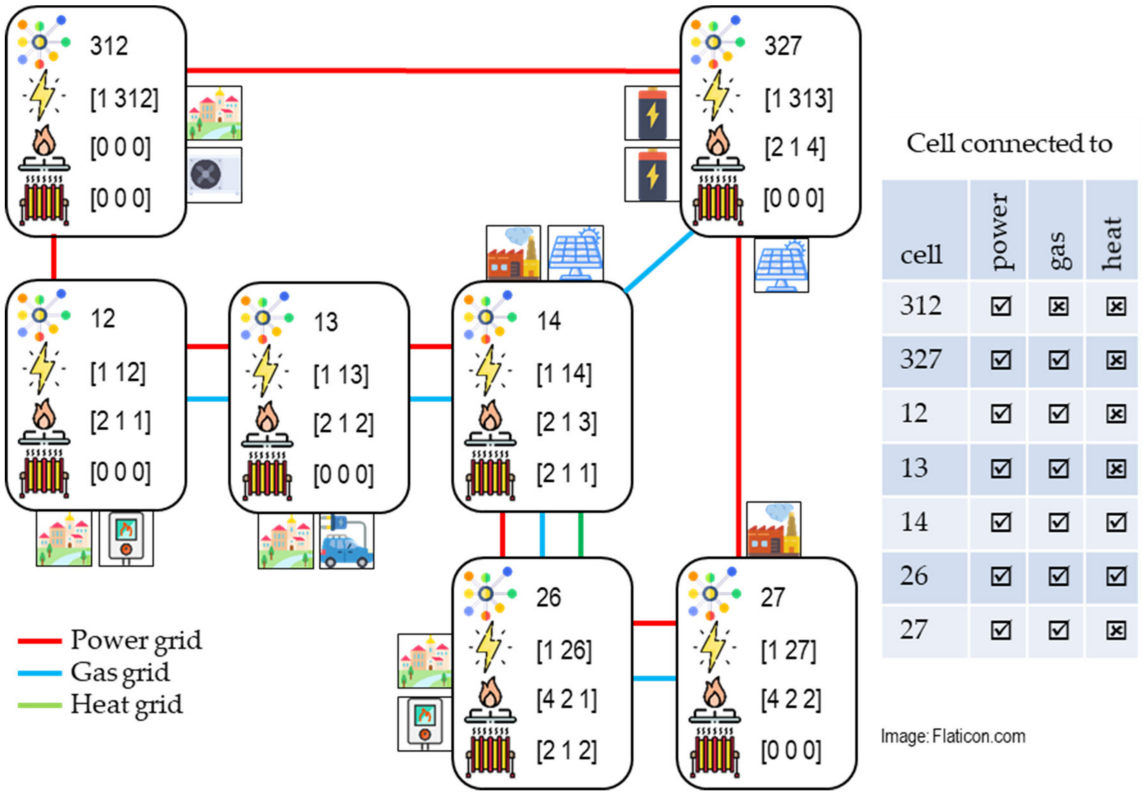

Figure 3. Energy infrastructure depiction.

To ensure that only the objects that are represented by an RL (refer to all classes hierarchically below "RL" in Figure 4) are addable to a RL collection, the programming principle of inheritance is used. A basic class "RL" is defined with simple properties (refer to Table 2 and functions. Based on the "RL" class, any derivative object can be developed and implemented by the user, with additional parameters to accommodate each object's individual need. Figure 4 displays available derivatives of the "RL" class. In each class, individual operating strategies can be implemented, depending on the user's need and addressed research question.

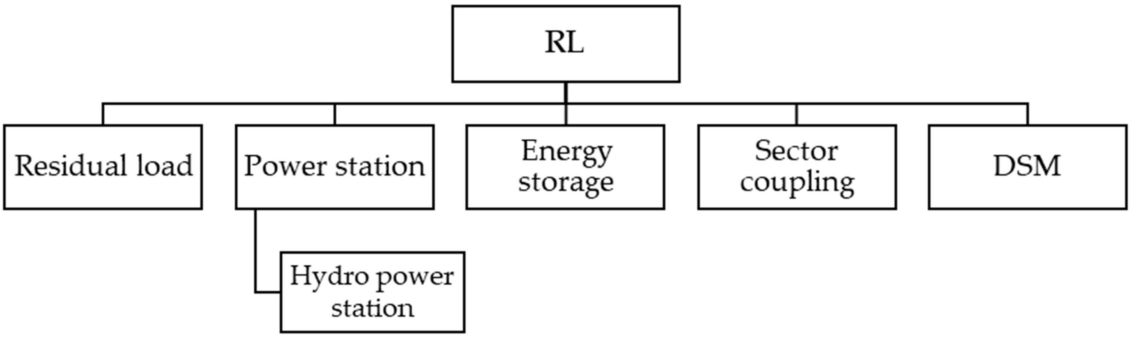

Figure 4. RL class and inherited derivatives.

Table 2. Overview of RL class properties.

Parameter	Description
type	Defines the type of underlying object. **Residual load or Power station** 1: Pre-defined residual load profile or power station with predefined temporally resolved profiles (e.g., residual load, water flowrate). **Sector coupling** 2: Power to gas and heat (PtGH). 3: Power to heat (PtH). 4: Heat to power (HtP). 5: Gas to heat (GtH). 6: Gas to power and heat (GtPH). **Energy storage** 7: Power storage. 8: Gas storage. 9: Heat storage. **DSM** 10: Electric vehicle. 11: Demand-side management.
RLgas	This vector contains the object's pre-set or calculated gas RL. The calculated gas RL depends on the object's operating strategy.
RLheat	Refer to RLgas.
RLpower	Like RLgas, except that active and reactive power RLs are considered.
RLgasFlex	These parameters contain the object's RL flexibility. The usage of these parameters depends on the object's operating strategy. The implementation of flexibility is explained in Section 2.1.4.
RLheatFlex	
RLpowerFlex	

2.1.2. Input Data

Before a simulation can be carried out in HyFlow, various input data need to be defined and read in for further processing. The input data are stored in individual objects, according to Table 2 and Figure 4. Node data must be defined, including parameters described in Table 1. Temporally resolved gas, heat, active, and reactive power RL data, including their associated node, can be defined. Properties for sector coupling options, storage, electric vehicle/DSM, and power stations (including their corresponding operating strategy) must be defined. Additionally, temporally resolved data for storage (e.g., water inflow in (pumped)-storage hydropower plant) are necessary. Properties include rated power, conversion or in-/output efficiencies, storage capacities, operating strategy, and further technology-specific properties.

Since the open-source power flow framework MATPOWER is used for power flow (PF) or optimal power flow (OPF) calculations, input data must reflect MATPOWER framework requirements. Therefore, tables for branch (=edge), bus (=node), generator, and generator cost data must be defined. The structure can be found in the MATPOWER documentation [25,26].

Gas and heat network properties follow the same principle scheme. For gas and heat, two tables need to be created. In the first sheet, connections between nodes at the same pressure level can be defined (e.g., between nodes 13 and 14 in Figure 3). The sheet number two contains connections between nodes at different pressure levels (e.g., between nodes 14 and 26 in Figure 3). Parameters are the gas or heat IDs of the connected nodes, length, diameter, roughness, and—in the case of heat—thermal conductivity of grid sections (edges).

2.1.3. Calculation Procedure and Grid Simulation

The calculation process of HyFlow is shown in Figure 5. The process of each dashed box will be explained further.

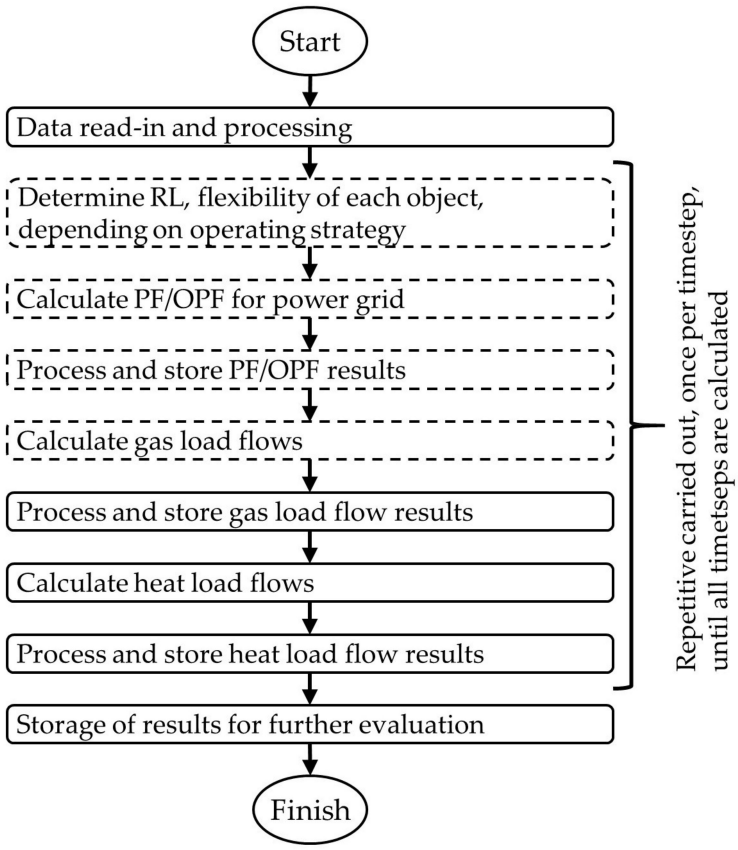

Figure 5. Overview of the calculation process.

Determination of RL

All objects in the RL collection of each specific node are assessed. Each object in the RL collection must provide an RL or flexibility based on the operating strategy of the object. The calculated summarized RLs and flexibilities of each node are transferred to the subsequent load flow calculations. The implementation and usage of flexibility are further explained in Section 2.1.4.

Power Grid PF or OPF

Depending on the users' selection MATPOWER PF or OPF, calculations can be performed for the power grid. Depending on the usage of PF or OPF, input data must be determined differently. In the case of PF simulation, all node residual loads and generator in-/outputs must be determined before a PF simulation can be performed. The PF simulation determines power load flows "as they physically are", without considering line restrictions or generation costs, for example. OPF mathematically optimizes load flows and generator dispatch, considering generation costs, line restrictions, and maximum/minimum generator power, based on the target function of minimum generation costs in the total power system [26]. Optimization restrictions, such as transmission line capacities or insufficient generation capacities, might cause an OPF to be incapable to converge. The advanced capabilities of OPF, compared to PF, come at the cost of higher complexity and increased likelihood of calculation failures. Further details regarding MATPOWER are provided in [26].

Before performing a PF or OPF calculation, bus (active and reactive power RL) and generator data (generation) must be updated in the MATPOWER data structure, based on the previous step's results (Determination of RL).

Gas and Heat Load Flow Calculation

Rüdiger adopts the node potential analysis for power grids in combination with Darcy's equation (refer to Equation (2)) to determine gas load flows [27].

$$\Delta p = \lambda \cdot \frac{8 \cdot \rho \cdot l \cdot \dot{V}^2}{d^5 \cdot \pi^2} \tag{2}$$

For heat load flows, Rüdiger's approach is extended by a second iteration loop to determine node temperatures and heat losses (refer to Equation (3) [28]) in both forward and return flow recursively.

$$T_{endnode} = (T_{startnode} - T_{ambient}) \cdot e^{\frac{-2 \cdot \pi \cdot k \cdot l}{c_p \cdot \rho \cdot \dot{V}}} + T_{ambient} \tag{3}$$

Both gas and heat load flow calculations can be characterized as steady-state load flow calculation approaches.

Process and Storage of Results

In the case of power OPF, MATPOWER determines each generator's generation based on minimum system generation costs. Therefore, the determined generation must be transferred to the corresponding object in the RL collection. The same procedure is necessary in case flexibilities are used. Depending on the energy carrier, further load flow calculation results such as load flows, voltage, angle, pressure, and temperature levels are stored.

2.1.4. Implementation and Usage of Flexibility Options

Power flexibility might generally accrue from sector coupling options, energy storage, or DSM, displayed by the yellow circles in Figure 6. Figure 6 also shows the general representation of each MES node, which is automatically adapted, depending on the properties of the node. A node optimization, similar to Chen et al. [29], is used to determine the node's flexibility band (green box in Figure 7) and usage of objects to provide flexibility (yellow box in Figure 7). Generally, node optimization aims to increase the profit of an MES (equal to minimizing costs), considering RL coverage, energy prices, technical properties of SC, and storage options [29]. This approach and its optimization target is adapted to determine the maximum/minimum power flexibility and the usage of objects providing flexibility, as explained further shortly.

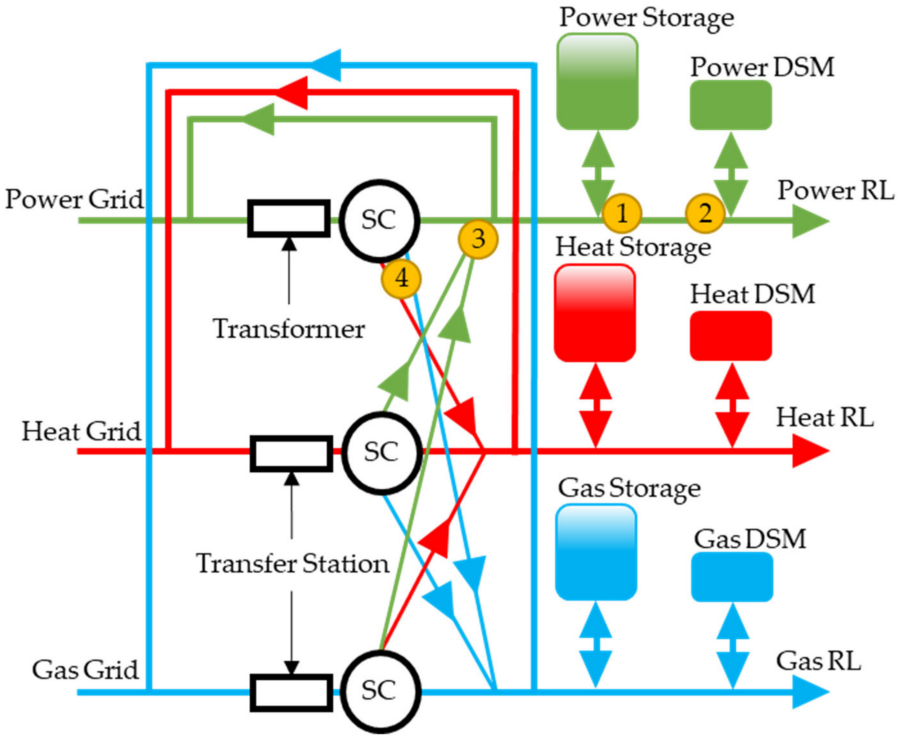

Figure 6. Generic node optimization representation.

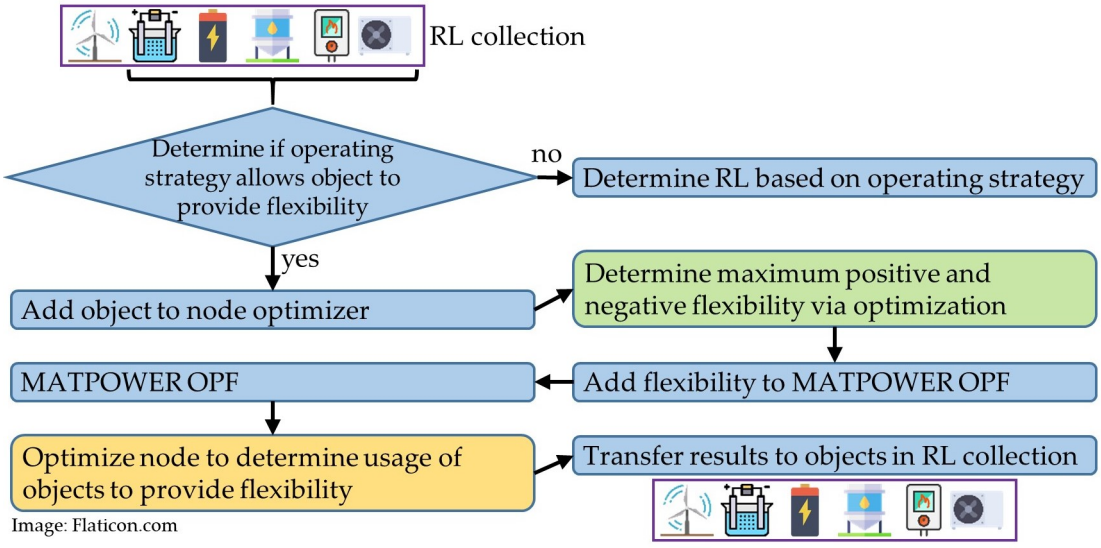

Figure 7. Process for optimized operating strategy, providing flexibility.

To consider flexibility in the HyFlow calculation process, the calculation process displayed in Figure 5 must be adapted. This adaption affects the upper three dashed boxes in Figure 5. The additional calculations to be performed are depicted in Figure 7.

If an object provides flexibility according to its operating strategy, it is considered for the following calculation procedure. If no flexibility is provided by the object, the RL is determined based on the objects operating strategy. To determine the total available flexibility per node, two optimizations are performed, aiming to determine the maximum possible positive and negative power RL (green box in Figure 7, target functions in Equations (A4) and (A5) in Appendix A), resulting in a flexibility band between both maximum and minimum power. For these optimizations, no energy prices are considered. The previously described calculation is carried out in the "Determine RL" section outlined in Figure 5.

Once a node's maximum positive and negative power flexibility is determined, it can be implemented in the MATPOWER framework as a generator at the corresponding node. The OPF, considering the whole depicted power system, determines the actual need for flexibility, ranging between the minimum and maximum possible flexibility of each node providing flexibility. So far, the need for flexibility at each node is determined; however, it is yet unknown which objects are used to what extent to provide the determined flexibility. To address this question, another node optimization is carried out (yellow box in Figure 7) to determine the actual usage of each object providing flexibility (target function in Equation (A1) in Appendix B). This optimization is carried out considering energy prices; therefore, the usage of the object is optimized economically. The determined optimal usage of each object providing flexibility is transferred to each corresponding object.

Yalmip [30] and Gurobi [31] are used to solve the optimization problems. Refer to "Appendix A. Node Optimization" for further mathematical details.

2.2. Austrian MES Modelling

The following modelling approaches are applied to develop an Austrian MES model. This includes an infrastructural depiction of power, natural gas, and heat grids, as well as timely and spatially resolved consumption and generation profiles.

2.2.1. Power Grid

The basis for the power grid model is a transmission grid plan. It shows the name of a substation's location and the transmission capacity of each line between substations for 110, 220, and 380 kV. However, the transmission grid plan only shows a past grid status. To determine a potential future power grid in 2030, potential grid expansion projects have to be included. The 220 and 380 kV transmission grid is operated by the Austrian Power Grid (APG), providing a grid development plan annually [32–37]. The 110 kV distribution grid is mainly owned and operated by nine local utilities in each federal state. Particularly for Upper Austria and Carinthia, detailed 110 kV grid expansion information is available [38,39]. Since the location of current and future substations and lines is roughly known, the geographic information system software QGIS [40], satellite images [41], and Open Street Map [42] are used to determine the exact location of substations and the course of power lines. MATPOWER requires line resistance, reactance, total line charging susceptance, and the maximum allowed apparent power flow [26]. APG provides detailed technical data for the transmission grid, which are used to parametrize the 220 and 380 kV grid [43]. The 110 kV grid is parametrized with literature values for resistance, reactance, and total line charging susceptance, as well as other already published projects [17,18,44,45], based on the maximum transmission current in the transmission grid plan.

2.2.2. Natural Gas Grid

To spatially depict Austria's natural gas infrastructure, we apply a similar approach compared to the power grid. Length and diameter for transnational pipelines and primary distribution system pipelines are available at Austrian Gas Grid Management (AGGM) [46]. The pipeline routing and length of national network level one (national transmission grid) and two (national distribution grid) can be derived from [47,48]. The diameter and pressure level are determined using statistical data [49], as well as information from utilities provided by request and previous projects [17]. Wall roughness is parameterized with the wall roughness of welded and seamless steel tubes [50].

2.2.3. Heat Grid

Currently, heat grids in Austria cover regional heat demand. Since the spatial resolution for an Austrian MES model is inadequate to depict regional heat grids, technical properties are assumed for interconnected regions, especially in urban areas. As a guideline, results from [51,52] are used to determine which areas of Austria are supplied with district heat.

2.2.4. Model of Austrian Natural Gas and Power Grid

Figure 8 displays the created model of Austria's power and natural gas infrastructure. It can be seen that the availability of Austria's energy infrastructure is much denser in urban and suburban areas in comparison to rural areas. Based on the infrastructure depiction in Figure 8 and Voronoi diagram methodology (refer to Section 2.2.5. Spatial Data Distribution), a corresponding node-edge model can be derived.

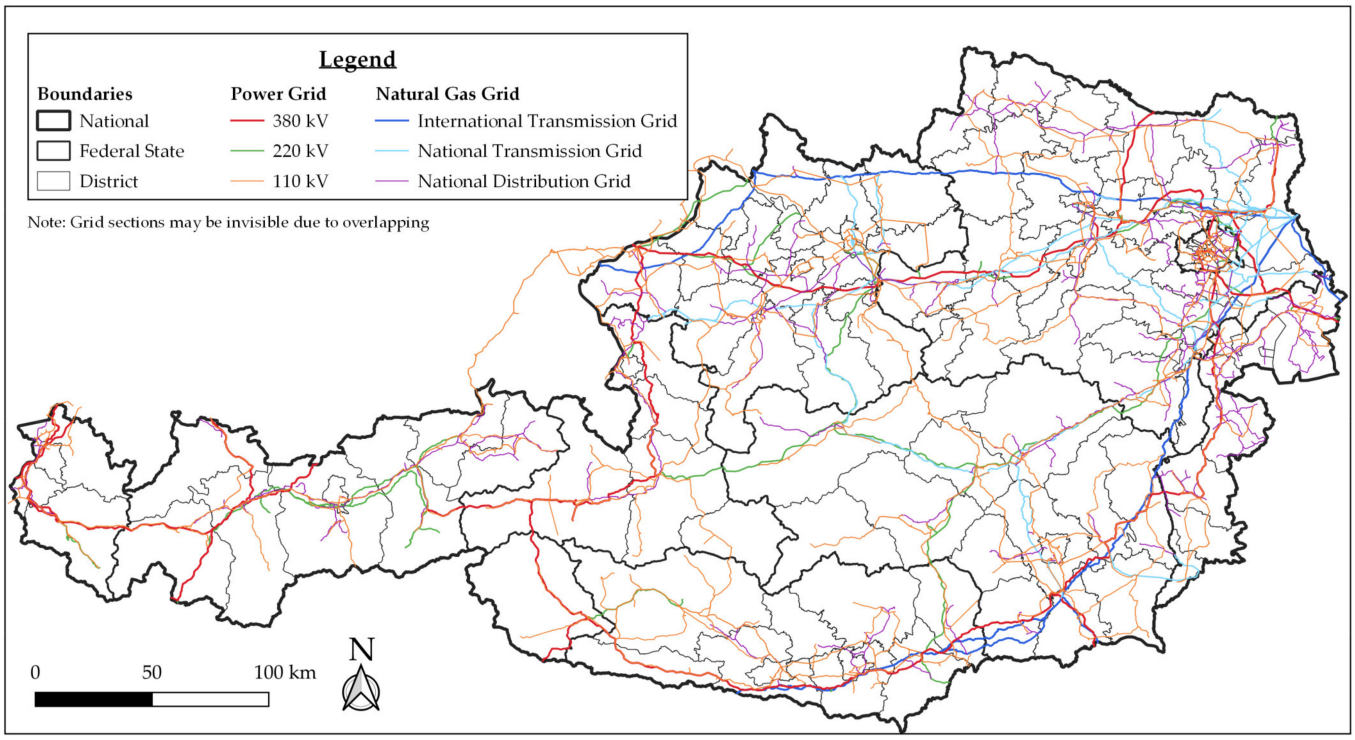

Figure 8. Model of Austria's power and natural gas infrastructure [9].

2.2.5. Spatial Data Distribution

To achieve a spatial resolution of Austria, a suitable methodology has to be selected to determine a spatial division of Austria. This is necessary to aggregate all objects (e.g., storage, power stations, RLs) within a spatial division into one node. A Voronoi diagram creates polygons starting from central points, dividing a layer into areas of equal nearest neighbors [53]. This approach is used with substations of the power grid as central points to determine single areas. The area covered by one substation is further referred to as a substation district (SSD). An example of the created SSDs within a selected area of Austria can be seen in Figure 13. In [8], the RES potentials of each Austrian community are determined. The RES potential data of each community are summed up to determine the SSD RES potential if a community is located within the boundaries of an SSD. Furthermore, power and natural gas (for both process and heating use) final energy consumption data from industrial, private, agricultural, and public and private service sectors are provided at a district level in [8]. To distribute final energy consumption data at the district level to a single community, the share of employees or households per community from *Statistik Austria*, in comparison to the district, is used [54]. Heat demand is modelled using the Austrian Heat Map [52]. Heat demand data are from 2012 but are quite stable till now [55]. Since heat demand data are available on a district level, and the same approach as for power and gas is used to distribute district demand to municipalities and then to SSDs. The useful energy analysis from *Statistik Austria* also provides information at the federal state level regarding the energy carrier used to provide heat [55].

2.2.6. Temporally Resolved Consumption Data

Annual energy consumption data of each SSD must be combined with temporally resolved load profiles to determine a temporally resolved RL profile for each SSD. For industrial power and gas demand, subsector specific load profiles are derived from [56]. For household, agriculture, and public and private service power consumption standardized load profiles (SLP) H0, L0, and G0 are used [57]. The reactive power is considered using literature and empiric values [58–60]. A cos(φ) of 0,98 is used. The temporal resolution of natural gas for non-heating purposes for households, agriculture, and service is determined based on the relatively steady cooking gas SigLinDe function [61]. The annual heating RL of each SSD is determined using the sectors corresponding SigLinDe function [61]. The temperature used as input data for the SigLinDe function is obtained for each SSDs substation from [62,63].

2.2.7. Temporally Resolved Generation Data

Oesterreichs Energie published a map of all power generation facilities in Austria with a power generation capacity greater than 10 MW [64,65]. In the following, we explain how each category of power station has been implemented into Austria's MES model.

Hydro Run-Off and Storage Power Station

The basic model of hydro run-off and storage power stations can be seen in Figure 9. Power generation is calculated using Equation (4) [66].

$$P = \eta \cdot \rho \cdot Q_{Turbine} \cdot g \cdot \Delta h \quad (4)$$

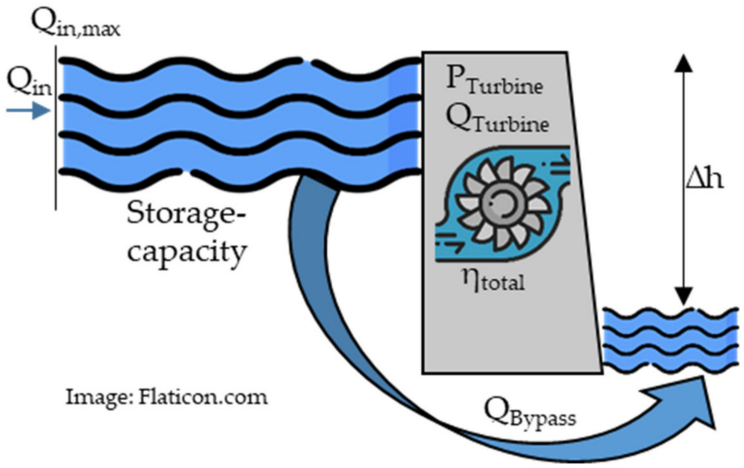

Figure 9. Hydro run-off and storage power plant model.

Each run-off and storage power station with a generation capacity greater than 10 MW is implemented into Austria's MES model in its corresponding SSD. Power station data are sourced from [67–79]. The temporally resolved generation is determined using run-off water measurements [80]. If the measurement point is different to the power station's location, interpolation is conducted between two measurement points. For hydropower stations with less than 10 MW, a different approach had to be used. *Kleinwasserkraft Österreich* [81] provides power and annual generation data for small-scale hydropower stations. These data are used together with hydropower potentials from [8] to determine small-scale hydropower in each SSD. Since no sufficient run-off measurements are available for small rivers, a standardized load profile based on measured data from small rivers (refer to Appendix B for measurement points) [80] is created, presented in Figure 10. A polynomial trend curve is used to smoothen the curve.

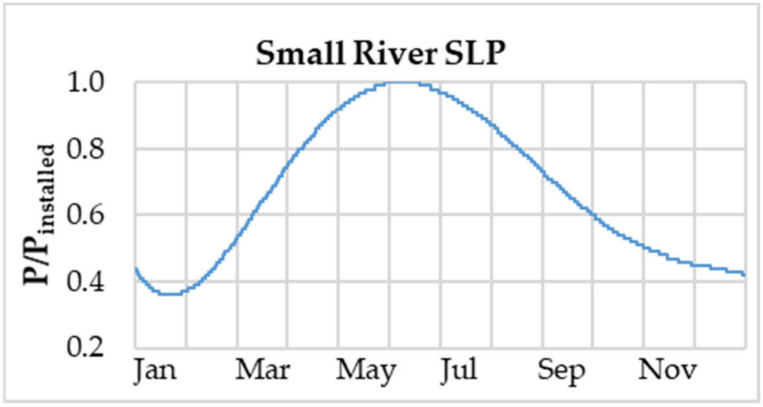

Figure 10. SLP small river, for small-scale hydro run-off power plants.

To cope with an additional 5 TWh of power, based on the government's RES expansion target [4], an increase in generation is carried out according to hydropower potentials from [82]. The small river SLP is used as a temporally resolved generation profile for these power stations.

(Pumped)-Storage Hydropower Plant

(Pumped)-storage hydropower plants are modelled as a simplified, flexible cascade of reservoirs, interconnected with pumps and turbines (refer to Figure 11).

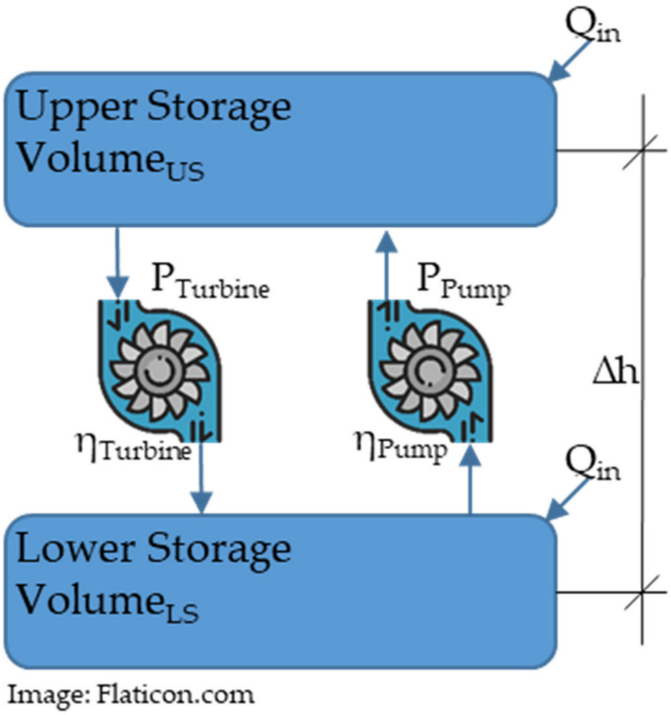

Figure 11. (Pumped)-storage hydropower plant model.

Technical properties such as storage capacity (Volume), annual inflow from natural sources (Q_{in}), and pump and turbine power ($P_{Turbine}$, P_{Pump}) are sourced from [68–70,73–76,79,82–84]. Furthermore, future projects such as [85,86] are considered as well. The pump (η_{Pump}) and turbine ($\eta_{Turbine}$) efficiency is set to 0.88 [87]. Reservoirs are naturally fed by water from glacier or snow melt. To determine a temporally resolved water inflow, suitable measurement data from [80] are used to derive an annual water inflow characteristic, displayed in Figure 12 (refer to Appendix C for measurement points). It can be seen that

the majority of natural inflow occurs during the summer months; in contrast, hardly any inflow can be expected in the winter months.

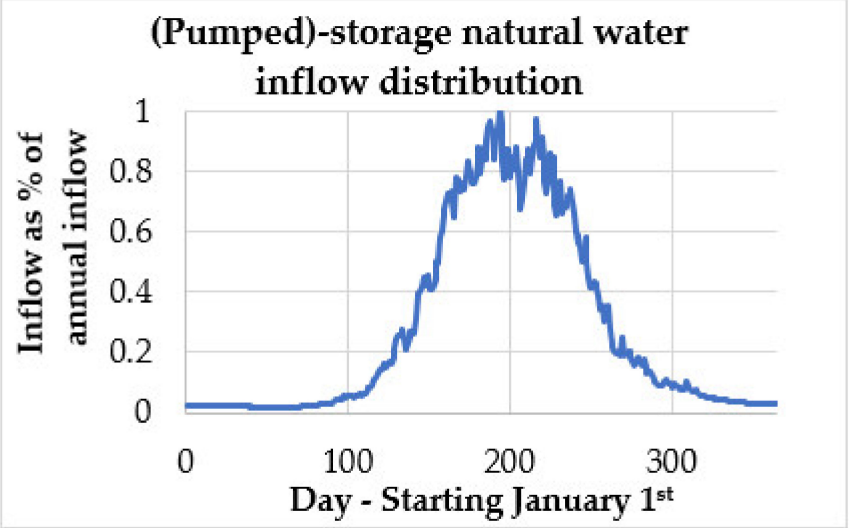

Figure 12. Annual (pumped)-storage hydropower plant natural inflow distribution.

The scenario-dependent generation and consumption profile for (pumped)-storage hydropower plants is described in the following chapter.

Biomass Combined Heat and Power (CHP) and Biogas Power Plants

Biomass CHP and biogas power plants are sourced from [88,89] and temporally resolved via SLP (E0) [57].

Photovoltaics

The installed photovoltaic power for each federal state is sourced from [90] and evenly distributed to each SSD via PV potentials from [8]. To reach the national goal of 11 TWh photovoltaics [4], photovoltaics are expanded, according to potentials in [8], by applying a split between rooftop and open area potentials of nine to one. Temporally resolved generation profiles are considered for each SSD, sourced from [62,63,91].

Wind

The locations of each wind park and their corresponding power levels are sourced from [92] and aggregated to the installed wind power of each SSD. To reach the national goal of 10 TWh wind power addition [4], the power at each SSD is evenly expanded according to potentials in [8]. Temporally resolved generation profiles are considered for each SSD, sourced from [62,63,93].

Thermal Generation

Technical data, such as power and efficiencies, of Austria's (combined cycle) gas turbine and large-scale CHP power plants are based on operators' publications [67,72,94–97]. If no efficiency data are available, an estimation based on comparable power plants is applied. The scenario-depended generation profile is described in the following chapter.

2.2.8. Power Exchange with Neighboring Countries

Power exchange with neighboring countries of Austria is considered based on data from *ENTSO-E*'s transparency platform for the year 2019 [98].

2.2.9. Example of Energy Infrastructure Depiction

An example of Austria's energy infrastructure and power plants can be seen in Figure 13. Exemplarily, an SSD is highlighted in yellow. The highlighted SSD contains several biogas plants and is connected to the power and natural gas grid. It can be seen that substations are concentrated in urban areas, whereas the substation density is lower in rural areas. More substations, compared to assignable municipalities, may especially occur in urban areas. In this case, suitable substations are manually selected and merged to create the Voronoi diagram. Hydropower plants are concentrated along large rivers, whereas wind, biomass CHP, and biogas are spread all over the area.

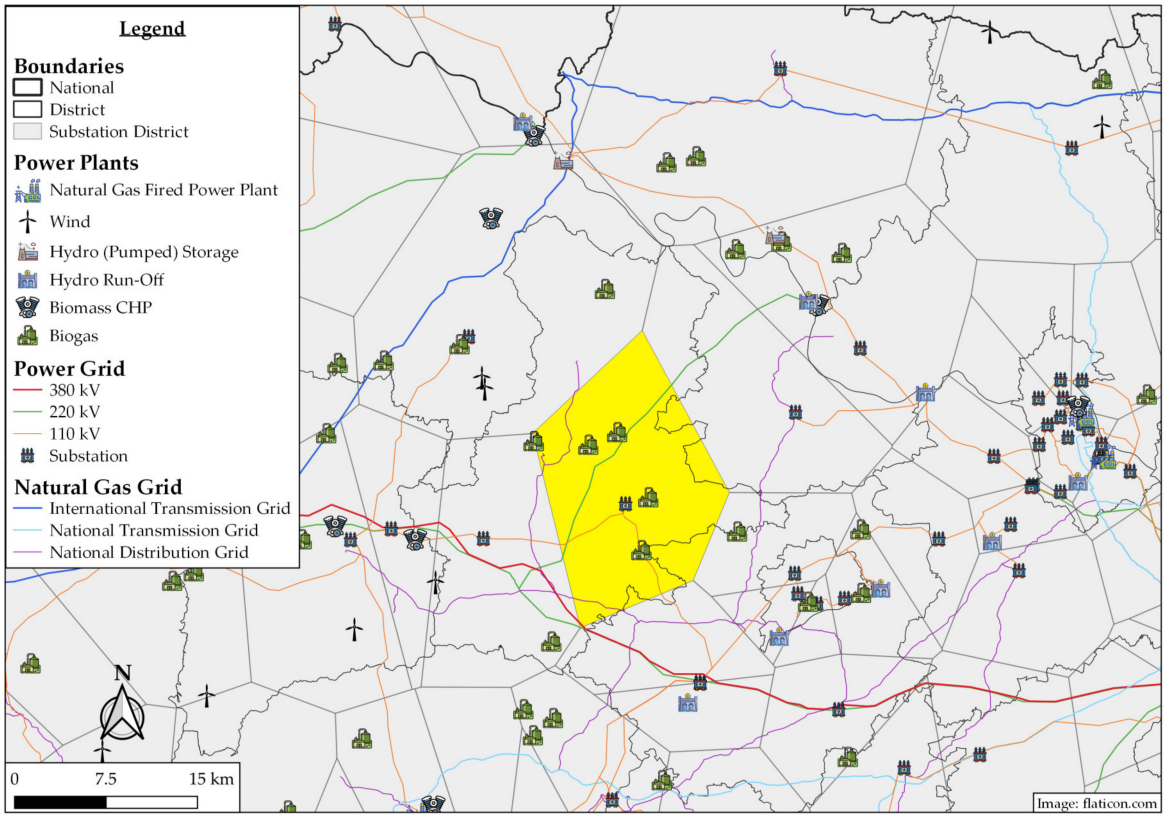

Figure 13. Example of Austria's energy infrastructure and power plants [9].

3. Scenarios

In this chapter, potential developments of the Austrian energy system are investigated based on three scenarios for the year 2030. Therefore, we apply the methodologies shown in Section 2. The following points are considered for each scenario:

- Since power, gas, and heat consumption are based on past data, sufficient studies need to be found to estimate the energy consumption in 2030. Austria's *Umweltbundesamt* (UBA) [99] estimates energy consumption in the years 2020, 2030, and 2050, based on the year 2015. Power demand is expected to remain stable between 2015 and 2020 and then increase between seven and thirty per cent, depending on the scenario. Electric vehicles, heat pumps, and electrolysis are seen as major drivers of power consumption growth. Since these consumers are additionally considered in each following scenario, we assume that the power demand will stay constant without. Depending on the scenario, a slight increase or decrease in natural gas consumption is assumed by *UBA*; therefore, we assume constant consumption [99]. Based on #mission2030 targets, thermal renovation of existing buildings should be doubled to two per cent per year, from current levels of around one per cent [5]. If a 50% heat demand reduction through a thermal renovation is assumed, heat demand might drop by thirteen per

cent, until 2030. The assumption of 50% heat demand reduction seems reasonable since subsidiaries are granted if more than 40% heat demand reduction is achieved [100]. The 13% heat reduction is between both *UBA* scenarios (WAM, WEM) for the final energy consumption of buildings [99].

- The number of electric vehicles in each SSD is determined based on vehicle registration data and trends in each federal state [101]. The share of electric vehicles in 2030 is expected to be 20%, based on scenarios in [102]. In Austria, a car is used for an average of 13,700 km per year. Based on the average consumption of 20 kWh/100 km, an annual electric energy demand per car of about 2750 kWh can be expected [103,104]. The temporal charging characteristic is scenario-dependent and can be explained in the following subchapters. All electric vehicles account for approximately 3 TWh of additional power consumption.
- The share of heat pumps for each SSD is determined based on the share of ambient heat usage for heating purpose divided by an assumed coefficient of performance of three [55]. Heat pump usage might increase by six-fold until 2030 based on [105]. The mode of operation depends on the scenario. All heat pumps account for approximately 1.9 TWh of additional power consumption.
- For every fourth household, battery energy storage with a storage capacity of 8 kWh, charging–discharging power of 2 kW, and an input–output efficiency of 90% [106] is implemented with a scenario-dependent mode of operation.
- Renewable energy sources are expanded according to plans of the federal government, shown in Table 3.

Table 3. Expansion of RES until 2030 [4,107].

RES	Generation 2018	Expansion Until 2030
Hydro	37.6 TWh	+5 TWh
Wind	6.0 TWh	+10 TWh
Photovoltaics	1.5 TWh	+11 TWh
Biomass	4.9 TWh	+1 TWh
Total	50 TWh	+27 TWh

Table 4 below provides an overview of the differences between each scenario. The modes of operation are explained in each scenario description.

Table 4. Scenario parameters.

	Scenario 1	Scenario 2	Scenario 3
Thermal generation and (pumped)-storage hydro	ENTSO-E	ENTSO-E	Flexibility
Electric vehicle	SLP	Optimized	Optimized
Battery storage	Greedy	Optimized	Optimized
Heat pump	Load following	Optimized with storage	Optimized with storage
Power grid calculation	PF	PF	OPF

3.1. Scenario 1—BAU

In this scenario, certain elements of the energy system are operated in the business-as-usual (BAU) mode. Electric vehicles are charged according to the SLP, derived from [108], with 3.7 kW charging power. Since the number of electric vehicles is above 1000 for the vast majority of substation districts, a low coincidence factor can be applied [108,109]. Heat pumps are operated as heat demand occurs, without a storage option. Temporal battery

storage behavior is determined as follows. The energy demand of an average household per SSD is coupled with an SLP (H0 [57]) and a 5 kW photovoltaic generation capacity, considering the SSDs' individual PV generation profile. One-quarter of households are equipped with battery storage. The battery storages operate according to the greedy algorithm to minimize the household energy demand from the power grid. Examples of the application of the greedy algorithm can be found in [110,111]. (Pumped)-storage hydropower and thermal power plants are operated according to *ENTSO-E* generation data from 2019 [98]. The resulting power RLs are added to each SSDs RL.

3.2. Scenario 2—Demand Optimization

Demand optimization is applied in this scenario to operate certain elements economically. An optimization concept similar to energy hubs is used to determine an economically optimized mode of operation of energy storage, heat pumps, and electric vehicles [29]. To enable a flexible operation of heat pumps, each heat pump is equipped with a thermal storage capacity of 50 kWh and a charging–discharging capacity of 10 kW. Electric vehicles charge their average daily consumption of about 7.5 kWh with 3.7 kW charging power. Peak demand times (6:00–9:00 and 17:00–20:00) are excluded from charging. The optimization is carried out, using power price data from 2019 [112] and each node's RL. As a result, price-optimal RLs of heat pumps, power storage, and electric vehicles are determined and added to each node's RLs.

3.3. Scenario 3—Demand Optimization and Flexibility

Heat pumps, electric vehicles, and battery power storage are operated, like in Scenario 2. Thermal power plants and (pumped)-storage hydropower plants are operated as additional flexibility (refer to Section 2.1.4). Since generation costs are considered in OPF for generator dispatch, the generation costs of each power source are set as follows:

- Subsidized forms of power generation, such as biogas, biomass CHP, wind, photovoltaics, and small-scale hydropower with 10 EUR/MWh;
- Large-scale hydropower 50 EUR/MWh;
- Flexibilities (gas turbine and CHP and (pumped)-storage hydropower) and import/export with 100 EUR/MWh.

4. Results

In all three discussed MES scenarios, natural gas and district heat grids show no critical overloads. Therefore, power grid results are discussed in detail. In Table 5, a comparison of overloaded distribution power grid (DG) and transmission power grid (TG) lines are displayed. Scenario 2 shows that the number of time steps, as well as affected power grid lines, increases compared to Scenario 1. This can be explained by the price-optimized mode of operation, since demand increases disproportionately in time steps with cheaper power, leading to RL peaks.

Table 5. Comparison of scenario results.

	Scenario 1	**Scenario 2**	**Scenario 3**
Overload time DG	182,205 time steps	206,592 time steps	81,991 time steps
Average DG line overload	38.8%	42.5%	35.5%
Count of overloaded DG lines	39/480	57/480	40/480
Overload time TG	3904 time steps	8131 time steps	144 time steps
Average TG line overload	16.0%	16.3	30.1%
Count of overloaded TG lines	5/104	7/104	6/104

To evaluate the degree of power line overloads, two different overloads are evaluated. As displayed in Figure 14, the average line overload and the top five per cent (based on the number of overloaded time steps) of line overloads are determined for each power grid line.

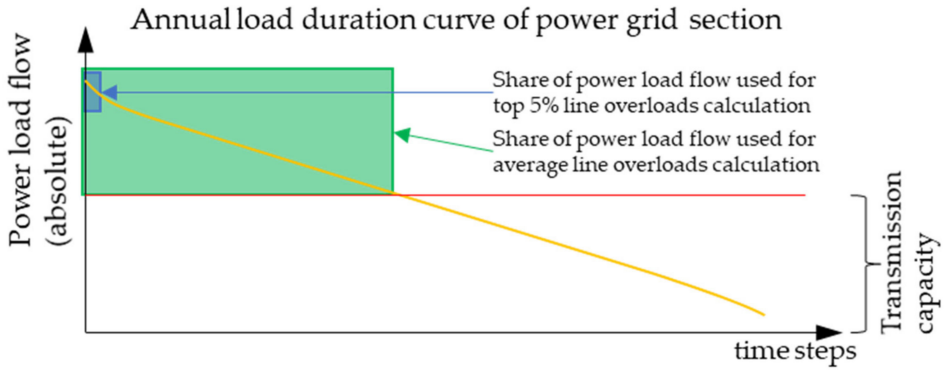

Figure 14. General determination of line overloads (an average and the top five per cent).

Subsequently, the worst (Scenario 2) and best (Scenario 3) case scenarios in terms of line overloads are displayed. In Figure 15, the average line loadings of Austria's power grid are displayed for Scenario 2. The thickness of each line qualitatively indicates the maximum transmission capacity of each line. Green lines indicate grid sections that are not affected by overloads. Orange to red lines indicate the average degree of overloads of the affected line section. Exemplarily, some grid sections are marked with a purple circle or ellipse-shaped indicators, allowing for the differentiation of the following overloads types:

- Continuous purple line—sections with low transmission capacity, e.g., single three-wire system;
- Dotted purple line—overloaded lines in urban areas;
- Dashed purple line—branch line with low transmission capacity in combination with either high potential of RES generation or demand;
- Dashed-dotted purple line—high potential of RES expansion.

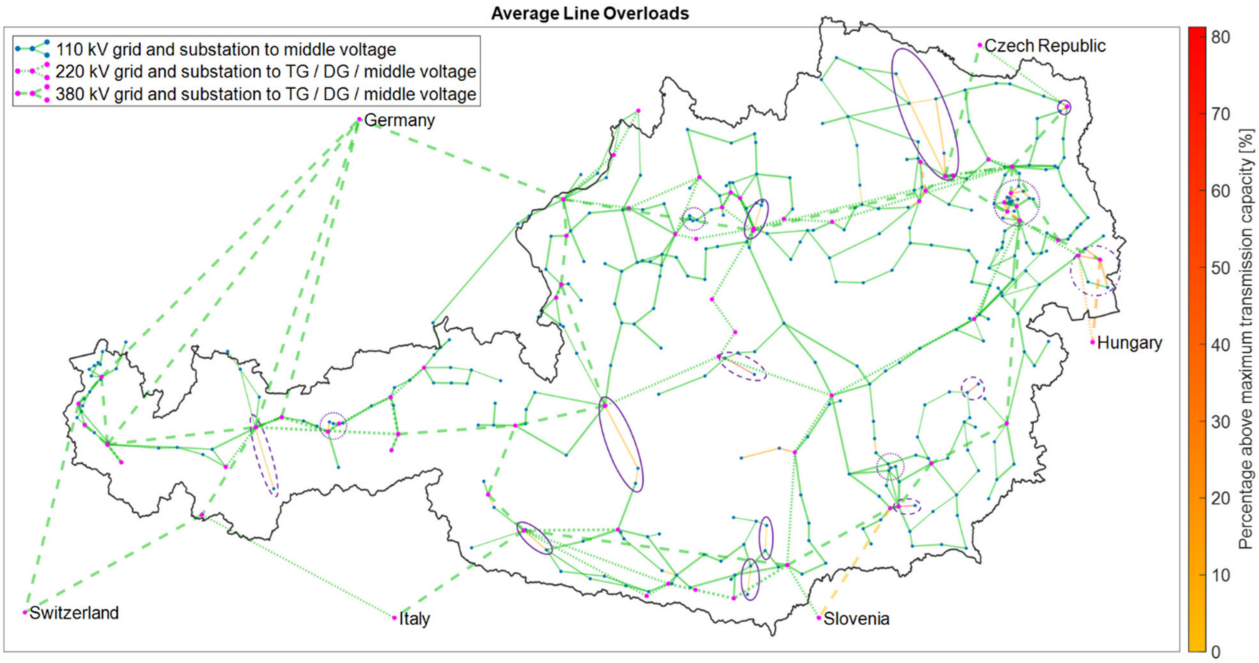

Figure 15. Average line overloads of Austria's power grid—Scenario 2.

In Figure 16, the top five per cent overloads of Austria's electricity grid are displayed for Scenario 2. It can be seen that most overloaded transmission and distribution grid lines are overloaded by a rather small degree.

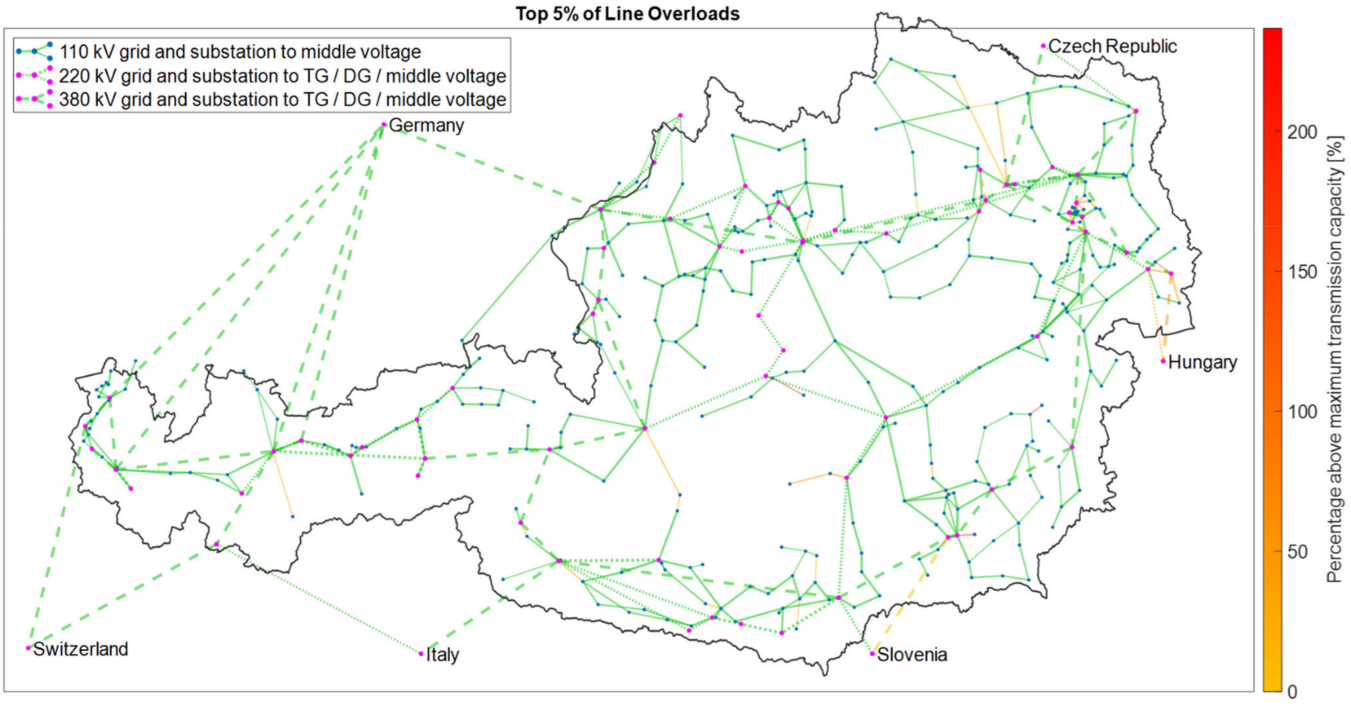

Figure 16. The top 5% line overloads of Austria's power grid—Scenario 2.

In following Figure 17 the annual load curve for a highly overloaded power branch line is displayed. It can be seen that the maximum transmission capacity is exceeded in both positive as well as negative direction. A positive and negative sign is related to the direction of power flow. This means that branch line overloads are caused by both consumptions at the end of the branch line and excess generation flowing from the end of the branch line towards the distribution grid.

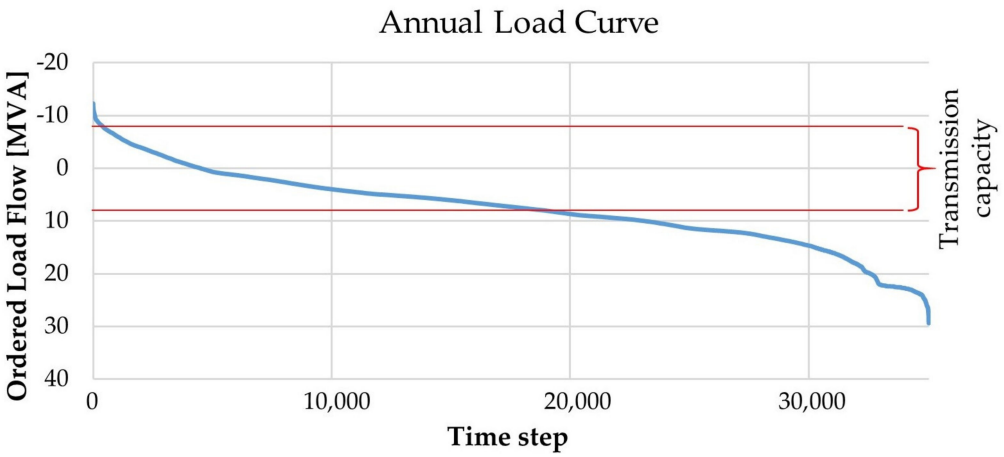

Figure 17. Annual load curve of a power branch line (ranked from min to max).

In Figure 18, the average power grid line overloads are displayed for Scenario 3. In comparison to Figure 15, the magnitude of the average overloads is significantly lower (refer to the scale magnitude). This observation is supported by line overload data displayed in Table 5, where line overloads in Scenario 3 are approximately halved in terms of

count, compared to Scenarios 1 and 2. A similar context can be observed by comparing Figures 16 and 19 where the magnitude of the top five per cent of overloads are significantly lower in Scenario 3, compared to Scenario 2.

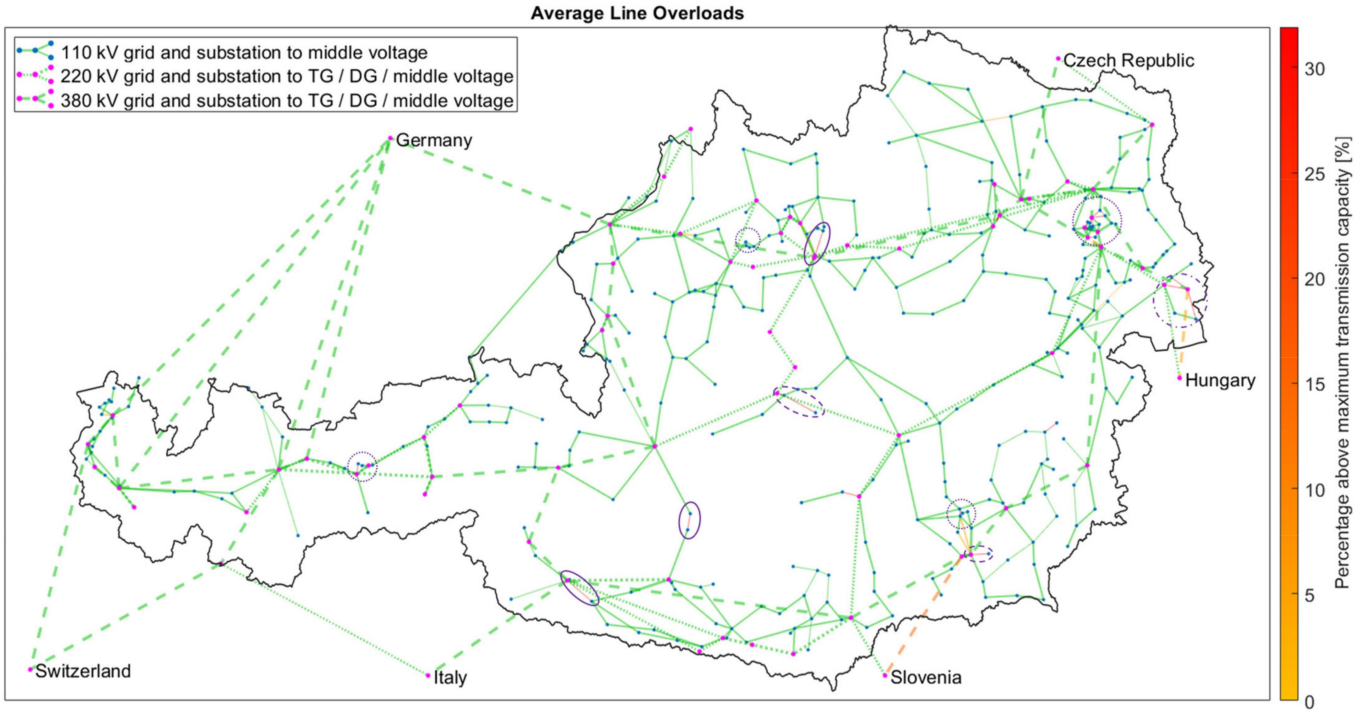

Figure 18. The average line overloads of Austria's power grid—Scenario 3.

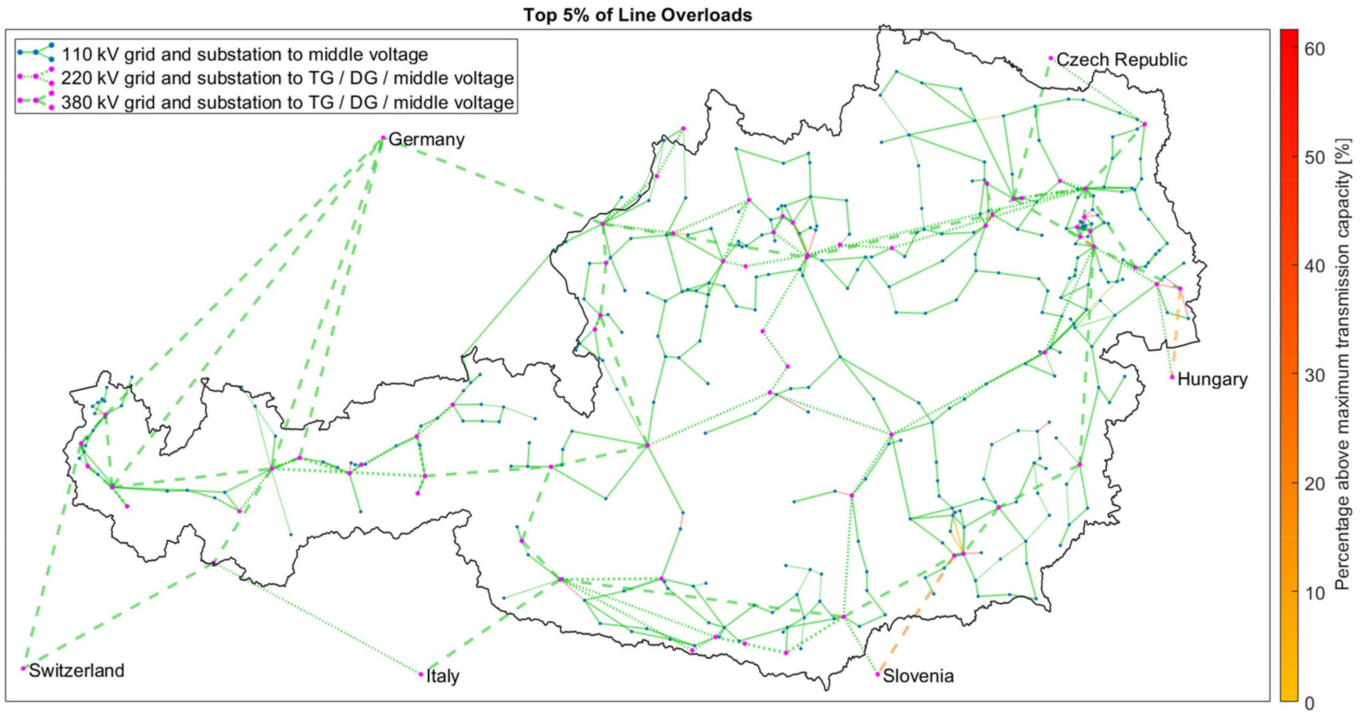

Figure 19. The top 5% line overloads of Austria's power grid—Scenario 3.

In Table 6, the power generation from each source is displayed for each scenario. It can be seen that the results for Scenarios 1 and 2 are identical, except for a small difference in imported and exported power. However, in Scenario 3, the generation from gas turbine

and CHP and (pumped)-storage hydropower is reduced by about fifty per cent compared to generations from Scenarios 1 and 2. The lower generation from both before-mentioned sources reduces power exports by about one third compared to Scenarios 1 and 2. The curtailment of generation occurs in Scenario 3 only, since OPF is used instead of PF for power load flow calculation to avoid line overloads. Imports and exports are calculated based on power line load flows connecting Austria with neighboring countries; therefore, the calculated power energy imports and exports do not consider loop flows.

Table 6. Comparison of power generation for each scenario.

	Scenario 1	**Scenario 2**	**Scenario 3**
Biomass	6.0 TWh	6.0 TWh	6.0 TWh
Photovoltaics	12.1 TWh	12.1 TWh	12.1 TWh
Wind	15.5 TWh	15.5 TWh	15.5 TWh
Gas turbine and CHP	10.8 TWh	10.8 TWh	Consumption: 0.83 TWh Generation: 8.2 TWh
(Pumped)-storage hydropower	Consumption: 1.5 TWh Generation: 8.5 TWh		
Hydropower >10 MW	27.9 TWh	27.9 TWh	27.9 TWh
Hydropower $\leq$10 MW	11.6 TWh	11.6 TWh	11.6 TWh
Import	8.1 TWh	10.5 TWh	3.7 TWh
Export	36.0 TWh	37.5 TWh	23.0 TWh

5. Discussion

In this section, we discuss the temporally and spatially resolved MES model of Austria, as well as the simulation results.

5.1. MES Model of Austria

Although Austria's #mission2030 aims for a net-balanced RES power supply over one year, depending on the applied scenario, significant power exports compared to imports are visible in Table 6 [5]. This gap can be explained exemplarily for Scenario 3 as follows. In Austria's MES model, power generation from company-owned CHP and power plants is not considered, since power is generated behind the meter and, therefore, company internally used. The internal generation reduces a company's power demand from the grid, as considered in the consumption data source [8]. This internal generation accounts for a total power generation of approximately 8 TWh [107]. The 7.5 TWh generation of the gas turbine and CHP has to be considered as well, since it is not a RES and therefore is not considered in the #mission2030 power generation target [5]. The remaining 3.8 TWh contain power grid losses, self-consumption of power plants, pumped-storage hydropower losses, variations of input data from [8], and others. This is in accordance with Austria's #mission2030.

The lack of subnational data available is seen as a main reason for a low spatial resolution in MES optimization projects [24]. These issues also present a main challenge within this work; however, based on experiences in [8], proven strategies are used to distribute aggregated data to more detailed granularity.

The Voronoi diagram is used because a more detailed approach may require further infrastructure data (e.g., roads) [113]. The Voronoi diagram does not take any local and geographical properties into account. Therefore, a community might be assigned to an SSD located across a mountain chain, for example. This case of misallocation is investigated manually since a small number of municipalities are affected. However, in this case, the municipalities are rather small in terms of energy consumption; therefore, the error of misallocation is considered to be negligible.

The usage of SLPs is valid if a number of several 100 consumers is aggregated [114]. This number is achieved for residential and to a smaller degree, for agricultural as well as public and private services consumers. The number of industrial consumers is significantly lower compared to the residential and service sectors. The quality of temporal consumption data can be further improved in the industrial sector, provided that more accurate industrial load profiles are available.

A temporal resolution of minutes to hours and days is common for MES frameworks which cover local levels up to regional and national levels [115]. This is important since the availability of data defines the achievable temporal resolution. For example, SLPs are available for 15 min (residential, agricultural, public, and private services) or, in the case of industrial SLPs, one-hour intervals. In comparison, wind and photovoltaic generation profiles are temporally resolved over one hour, whereas water flow rates, used to calculate hydropower plants generation, are available as daily averages. Although the simulation is carried out in 15 min interval time steps, a one-hour time step might be considered in the future to decrease computation time. Generally, simulating an MES system of the displayed size for a full year in 15 min's interval time steps takes approximately 2 days of calculation time. If node optimization is used additionally (Scenario 3), the computation time increases further.

5.2. Simulation Results

As displayed in Table 5, line overloads can be significantly reduced by more than fifty per cent in Scenario 3 compared to Scenarios 1 and 2, showing a positive effect of OPF and flexibility usage. Transmission line capacities represent a constraint using OPF applied in Scenario 3, therefore a number of zero line overloads should be expected. However, based on simulation results from Scenarios 1 and 2, the capacity of overloaded power grid sections is increased to enable the OPF to converge, since any unsolvable violation of transmission capacity would result in a termination of an OPF calculation. The count of the overload time for Scenario 3 is carried out using the original transmission capacity used in Scenario 1 and 2, considering the load flow occurring with increased line capacity.

Depending on the scenario, more than ninety-five per cent of line overloads occur in the distribution grid. Overloads can be caused by various reasons such as high RES potentials, low transmission capacity or in urban areas. No clear reason could be identified for overloads in urban areas. Potential issues might arise from the data source (consumption data) or loss of precision due to the need for grid simplification in urban areas.

In Scenario 3, the export of power is reduced significantly in comparison to Scenarios 1 and 2, since the power generation from natural gas CHP, gas turbine and especially (pumped)-storage hydropower plants is reduced. This is achieved by operating gas turbine and CHP, and (pumped)-storage hydropower plants as dispatchable flexibility. Since (pumped)-storage hydropower plants are located in western Austria and gas CHP and turbine are close to cities (=high power consumption), natural gas CHP and turbine are more likely to be activated due to lower transmission losses. This point can be further addressed through different flexibility pricing to favour (pumped)-storage hydropower usage over natural gas turbine and CHP power plants. However, this might have effects on the west–east power transmission in Austria's power grid.

6. Conclusions and Future Outlook

Within this work, we introduce a unique MES simulation framework and investigate the effects of the expansion of renewable energy sources on Austria's energy infrastructure based on a created MES model within this work.

The literature review has shown that current available multi-energy system simulation and optimization frameworks are not capable of depicting a national MES with a high degree of both high spatial and timely resolution. To overcome this scientific gap, the updated MES simulation framework HyFlow is introduced. The proposed MES simulation framework is capable of implementing the energy carrier power, natural gas and district

heat (and their corresponding energy grid infrastructure), a broad range of individual consumers and producers, as well as storage and sector coupling options. Due to the flexible MES depiction approach, a wide range of research questions can be addressed. We believe that the HyFlow framework is unique in both existing and potential expansion capabilities and should be used to address various further research questions. This may include the addition of further capabilities to be added to the existing MES framework, such as further modes of operation, new objects, or improved gas and heat load flow calculations.

To depict a national MES, three main points must be addressed. First, detailed energy infrastructure models must be available. Due to the unavailability of Austria's energy grid infrastructure models, sufficient available sources and data from existing research are used to create a detailed model of Austria's energy infrastructure. Second and third, the examined area must be fed with both spatial and time-resolved consumption and generation data. To spatially resolute Austria, Voronoi diagrams based on power grid substations are used to divide Austria into so-called substation districts. To time-resolve the energy demands and generations of each substation district, a combination of SLPs and real-measured data is used. The created MES model of Austria may serve as a foundation for any further assessments of the Austrian MES. Potential fields could be the implementation of further flexibilities (e.g., storage and sector coupling) or assessment of other energy grids (gas, heat). If detailed RES expansion plans are available, the spatial distribution of RES expansion can be updated and its effects on energy grid infrastructure can be further investigated. New energy grid projects can be added to increase the transmission capacity between SSDs. We believe that this demonstrated approach can be a useful guideline to create a spatially and temporally resolved model of any national or regional MES.

Based on the created MES model of Austria and the presented MES simulation framework HyFlow, three scenarios are examined. The scenarios investigate the effects of Austrian government targets to achieve a one hundred per cent renewable power generation, net-balanced over one year. Renewable generation is expanded (mainly volatile wind and photovoltaics) by the aimed amount of the Austrian government. Additionally, electric vehicles, battery storage, and heat pumps are implemented into the MES simulation to an expectable future degree. Each scenario considers the same renewable expansion but differentiates between modes of flexibilities operation, such as (pumped)-storage hydropower, gas-fired power plants, heat pumps, electric vehicles, and battery storage. Results show that the mode of operation of flexibilities and the power load flow calculation methodology (PF and OPF) can lead to significantly different results, in terms of power line overload counts. By optimizing the consumption and generation of electric vehicles, battery storage and heat pumps based on the power price timeline (=market oriented), short demand peaks can occur, leading to the highest count of power grid overloads of all three investigated scenarios. In contrast, using OPF in combination with the flexible dispatch of natural gas-fired and (pumped)-storage hydropower plants line overloads are reduced by more than fifty per cent. The usage of OPF is therefore advantageous in contrast to PF, in terms of flexibility usage. It can be concluded that a solely price-optimized operation (market oriented) leads to grid overloads due to the neglectance of the power grids' transmission capacities. Therefore, both market and energy grid transmission capacity should be considered. A high degree of flexibilities, in a grid-supporting operation, are favorable to mitigate power grid overloads. Potentially, the addition of further flexibilities might have further positive impacts on the power grid.

Author Contributions: Conceptualization: M.G. and T.K.; methodology, software, validation, and formal analysis: M.G., F.F., J.S., N.Z. and N.W.W.; data curation: M.G., F.F., J.S., N.W.W. and T.S.; writing—original draft preparation: M.G.; writing—review and editing: N.W.W. and T.K.; visualization, M.G. and N.W.W.; supervision, T.K. All authors have read and agreed to the published version of the manuscript.

Funding: This research received no external funding.

Conflicts of Interest: The authors declare no conflict of interest.

Abbreviations

APG	Austrian Power Grid
CHP	combined heat and power
DG	distribution grid
EC	energy carrier
GtH	gas to heat
GtPH	gas to power and heat
HtP	heat to power
MES	multi-energy system
MESS	multi-energy system simulator
OPF	optimal power flow
PF	power flow
PtGH	power to gas and heat
PtH	power to heat
RES	renewable energy source
RL	residual load
SC	sector coupling
SLP	standardized Load Profile
SSD	sub-station district
TG	transmission grid
UBA	Umweltbundesamt (Federal Environment Agency)

Appendix A. Node Optimization

The node optimization and flexibility determination can be depicted in a four-stage process, displayed in Figure A1. Main parameters are explained in the following subchapters.

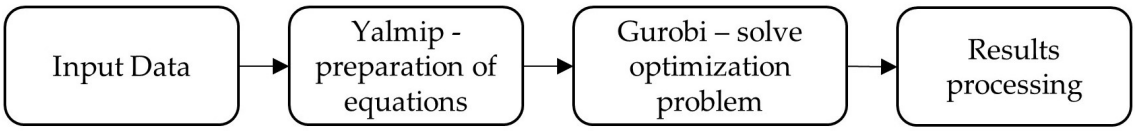

Figure A1. Optimization process.

Appendix A.1. Input Data

In Table A1, the input data for node optimization and flexibility determination are explained. Depending on the optimization problem, different input data are required. The optimization is adapted based on [29].

Table A1. Optimization input data.

Parameter	Type	Description
P_RL_Set	scalar	Residual load setting for the current time step.
t	scalar	Duration of one time step [h].
Converter	matrix	Defines properties of each converter. Each row represents one converter. [*FP*, *FH*, *FG*, *TP*, *TH*, *TG*, *MinP*, *MaxP*, *Ramp*, *PPrevPeriod*] *FP*—convert from power (1 or 0). *FH*—convert from heat (1 or 0). *FG*—convert from gas (1 or 0). *TP*—convert to power (η in [1]). *TH*—convert to heat (η in [1]). *TG*—convert to gas (η in [1]). *MinP*—minimum power [W]. *MaxP*—maximum power [W]. *Ramp*—ramp rate based on MaxP. *PPrevPeriod*—power of previous period [W].
P_Storage *H_Storage* *G_Storage*	matrix	Defines properties of each storage. Each row represents one storage. For power, heat, and gas, individual matrices have to be set up with the following structure. [*LP*, *MinSL*, *MaxSL*, *ISL*, *ηIn*, *MinIn*, *MaxIn*, *ηOut*, *MinOut*, *MaxOut*] *LP*—storage loss per period [1/h]. *MinSL*—minimum allowed storage level [Wh]. *MaxSL*—maximum allowed storage level [Wh]. *ISL*—initial storage level [Wh]. *ηIn*—input efficiency [1]. *MinIn*—minimum input power [W]. *MaxIn*—maximum input power [W]. *ηOut*—output efficiency [1]. *MinOut*—minimum output power [W]. *MaxOut*—maximum output power [W].
P_DSM *H_DSM* *G_DSM*	matrix	Defines properties of each DSM. Each row represents one DSM. For power, heat, and gas, individual matrices have to be set up with the following structure. [*MinP*, *MaxP*] *MinP*—minimum feed-in (demand) or maximum feed-out (generation) power. *MaxP*—maximum feed-in (demand) or minimum feed-out (generation) power.
eVehicle	vector	Defines parameters for electric vehicles. [*EC*, *CP*, *NoP*, *SB_1*, *EB_1*, *SB_2*, *EB_2*] *EC*—energy to be charged within *NoP* [Wh]. *CP*—charging power [W]. *NoP*—number of time steps before charging of EC must be finished (e.g., one day). *SB_1*, *SB_2*—the start of the charging break period. *EB_1*, *EB_2*—the end of the charging break period.
P_Price *H_Price* *G_Price*	vector	The number of rows is equivalent to the forecasting period. A separate vector must be defined for each energy carrier's price.
P_RL *H_RL* *G_RL*	vector	The number of rows is equivalent to the forecasting period. A separate vector must be defined for each energy carrier's residual load [W].
G_Connect *H_Connect*	scalar	Indicates if the node is connected (variable = 1) to gas/heat grid or not (variable = 0).
ops	vector	Contains settings for the Gurobi optimizer.

Appendix A.2. Node Optimization Target Function (TF)

$$TF = min(\sum_{EC}^{P,H,G}\left(\left(P_{EC} - P_{EC}^{€}\right)\cdot EP_{EC}\cdot t\right)) \quad \text{(A1)}$$

P_{EC}—consumed power for each energy carrier (EC).
$P_{EC}^{€}$—feed-in (sold) power for each EC.
EP_{EC}—price of EC.

Appendix A.3. Flexibility Determination Target Function

Positive and negative flexibility is determined according to (A2) and (A3).

$$TF_{Flex,\ neg} = \max(P_{C,out}) \quad \text{(A2)}$$

$P_{C,out}$—power converter power output.

$$TF_{Flex,\ pos} = \max(P_{C,in}) \quad \text{(A3)}$$

$P_{C,in}$—power converter power input.

To determine the total positive (A4) and negative flexibility (A5), storage and DSM options also have to be considered.

$$Flex_{pos} = TF_{Flex,\ pos} + \min\left(MaxIn, \frac{MaxSL - ISL}{t\cdot\eta IN}\right) + DSM_{MaxP} \quad \text{(A4)}$$

$$Flex_{neg} = TF_{Flex,\ neg} + \min\left(MaxOut, \frac{ISL\cdot\eta Out}{t}\right) + DSM_{MinP} \quad \text{(A5)}$$

Appendix A.4. Results

The main optimization outputs are time-resolved RLs for each converter, storage, and DSM, as well as specific results such as storage level. Furthermore, an additional parameter indicates if the optimization problem can be solved successfully.

Appendix B. Measurement Points for Small Hydropower Plant SLP

For each federal state, a random small river measurement point from [80] is used to create an SLP for small-scale hydropower plants, as displayed in Table A2.

Table A2. Measurement points used for small hydropower plant SLP [80].

Federal State	Measurement Point #	Name
Vorarlberg	200105	Garsella
Tyrol	230706	In der Au
Salzburg	203265	Schweighofbrücke
Carinthia	213389	Kaunz
Styria	211029	Anger
Upper Austria	204784	Riedau
Lower Austria	208041	Hollenstein
Burgenland	210039	Piringsdorf (Pfarrbrücke)
Vienna	None	None

Appendix C. Measurement Points for Natural Inflow Curve for (Pumped)-Storage Hydropower Plants

Natural water inflow into (pumped)-storage hydropower plants originates from water sources at high altitudes, such as snow and glacier melt. Therefore, measurement points from [80] at high elevation are selected to determine an annual inflow characteristic for (pumped)-storage hydropower plants, as displayed in Table A3.

Table A3. Measurement points used for annual (pumped)-storage hydropower plant inflow SLP [80].

Measurement Point Name	Measurement Point #	Elevation [m]
Gepatschalm	230300	1895
Vent (oberhalb Niedertalbach)	201350	1891
Obergurgl	201376	1879
Neukaser	201996	1786
Innergschlöß	212068	1686
Kees	203893	2040

References

1. European Commission. The European Green Deal, Brussels, 2019. Available online: https://eur-lex.europa.eu/resource.html?uri=cellar:b828d165-1c22-11ea-8c1f-01aa75ed71a1.0002.02/DOC_1&format=PDF (accessed on 12 January 2022).
2. European Commission. What is the European Green Deal? Brussels, 2019. Available online: https://ec.europa.eu/commission/presscorner/detail/en/fs_19_6714 (accessed on 12 November 2021).
3. European Commission. Fit for 55: Delivering the EU's 2030 Climate Target on the Way to Climate Neutrality, Brussels, 2021. Available online: https://eur-lex.europa.eu/legal-content/EN/TXT/PDF/?uri=CELEX:52021DC0550&from=DE (accessed on 12 November 2021).
4. Bundeskanzleramt. Aus Verantwortung für Österreich: Regierungsprogramm 2020–2024, Wien, 2020. Available online: https://www.bundeskanzleramt.gv.at/dam/jcr:7b9e6755-2115-440c-b2ec-cbf64a931aa8/RegProgramm-lang.pdf (accessed on 11 November 2021).
5. Bundesministerium Nachhaltigkeit und Tourismus; Bundesministerium Verkehr Innovation und Technologie. #Mission2030: Die Österreichische Klima- und Energiestrategie, Wien, 2018. Available online: https://www.bundeskanzleramt.gv.at/dam/jcr:903d5cf5-c3ac-47b6-871c-c83eae34b273/20_18_beilagen_nb.pdf (accessed on 12 January 2022).
6. Mancarella, P. MES (multi-energy systems): An overview of concepts and evaluation models. *Energy* **2014**, *65*, 1–17. [CrossRef]
7. Hansen, K.; Breyer, C.; Lund, H. Status and perspectives on 100% renewable energy systems. *Energy* **2019**, *175*, 471–480. [CrossRef]
8. Sejkora, C.; Kühberger, L.; Radner, F.; Trattner, A.; Kienberger, T. Exergy as Criteria for Efficient Energy Systems—A Spatially Resolved Comparison of the Current Exergy Consumption, the Current Useful Exergy Demand and Renewable Exergy Potential. *Energies* **2020**, *13*, 843. [CrossRef]
9. Bundesamt für Eich- und Vermessungswesen. *Katalog Verwaltungsgrenzen (VGD)—Stichtagsdaten 1:5000*; Bundesamt für Eich- und Vermessungswesen: Wien, Austria; Available online: https://www.data.gv.at/katalog/dataset/bev_verwaltungsgrenzenstichtagsdaten150000 (accessed on 15 February 2022).
10. Klemm, C.; Vennemann, P. Modeling and optimization of multi-energy systems in mixed-use districts: A review of existing methods and approaches. *Renew. Sustain. Energy Rev.* **2021**, *135*, 110206. [CrossRef]
11. Pfenninger, S.; Hawkes, A.; Keirstead, J. Energy systems modeling for twenty-first century energy challenges. *Renew. Sustain. Energy Rev.* **2014**, *33*, 74–86. [CrossRef]
12. Bottecchia, L.; Lubello, P.; Zambelli, P.; Carcasci, C.; Kranzl, L. The Potential of Simulating Energy Systems: The Multi Energy Systems Simulator Model. *Energies* **2021**, *14*, 5724. [CrossRef]
13. Lohmeier, D.; Cronbach, D.; Drauz, S.R.; Braun, M.; Kneiske, T.M. Pandapipes: An Open-Source Piping Grid Calculation Package for Multi-Energy Grid Simulations. *Sustainability* **2020**, *12*, 9899. [CrossRef]
14. Weinand, J.M.; Scheller, F.; McKenna, R. Reviewing energy system modelling of decentralized energy autonomy. *Energy* **2020**, *203*, 117817. [CrossRef]
15. Thurner, L.; Scheidler, A.; Schafer, F.; Menke, J.-H.; Dollichon, J.; Meier, F.; Meinecke, S.; Braun, M. Pandapower—An Open-Source Python Tool for Convenient Modeling, Analysis, and Optimization of Electric Power Systems. *IEEE Trans. Power Syst.* **2018**, *33*, 6510–6521. [CrossRef]
16. Böckl, B.; Greiml, M.; Leitner, L.; Pichler, P.; Kriechbaum, L.; Kienberger, T. HyFlow—A Hybrid Load Flow-Modelling Framework to Evaluate the Effects of Energy Storage and Sector Coupling on the Electrical Load Flows. *Energies* **2019**, *12*, 956. [CrossRef]
17. Kienberger, T.; Traupmann, A.; Sejkora, C.; Kriechbaum, L.; Greiml, M.; Böckl, B. Modelling, designing and operation of grid-based multi-energy systems. *Int. J. Sustain. Energy Plan. Manag.* **2020**, *29*, 7–24. [CrossRef]

18. Greiml, M.; Fritz, F.; Kienberger, T. Increasing installable photovoltaic power by implementing power-to-gas as electricity grid relief—A techno-economic assessment. *Energy* **2021**, *235*, 121307. [CrossRef]
19. FFG. SBM_Ind: Smart Business Models for Industry. Available online: https://projekte.ffg.at/projekt/3093356 (accessed on 13 November 2021).
20. Farshidian, B.; Ghahnavieh, A.R. A comprehensive framework for optimal planning of competing energy hubs based on the game theory. *Sustain. Energy Grids Netw.* **2021**, *27*, 100513. [CrossRef]
21. Cheng, Y.; Zhang, P.; Liu, X. Collaborative Autonomous Optimization of Interconnected Multi-Energy Systems with Two-Stage Transactive Control Framework. *Energies* **2020**, *13*, 171. [CrossRef]
22. Sejkora, C.; Kühberger, L.; Radner, F.; Trattner, A.; Kienberger, T. Exergy as criteria for efficient energy systems—Maximising energy efficiency from resource to energy service, an Austrian case study. *Energy* **2022**, *239*, 122173. [CrossRef]
23. Wagner & Elbling GmbH. ONE100: Österreichs Nachhaltiges Energiesystem—100% Dekarbonisiert, Wien, 2021. Available online: https://www.aggm.at/files/get/b2327a5f19bc53c7fa0f2ae1dcd4edb1/ONE100_Kurzfassung.pdf (accessed on 14 November 2021).
24. Aryanpur, V.; O'Gallachoir, B.; Dai, H.; Chen, W.; Glynn, J. A review of spatial resolution and regionalisation in national-scale energy systems optimisation models. *Energy Strategy Rev.* **2021**, *37*, 100702. [CrossRef]
25. Zimmerman, R.D.; Murillo-Sanchez, C.E.; Thomas, R.J. MATPOWER: Steady-State Operations, Planning, and Analysis Tools for Power Systems Research and Education. *IEEE Trans. Power Syst.* **2011**, *26*, 12–19. [CrossRef]
26. Zimmerman, R.D.; Murillo-Sánchez, C.E. MATPOWER User's Manual: Version 7.1. 2020. Available online: https://matpower.org/docs/MATPOWER-manual.pdf (accessed on 15 December 2021).
27. Rüdiger, J. Enhancements of the numerical simulation algorithm for natural gas networks based on node potential analysis. *IFAC-Pap.* **2020**, *53*, 13119–13124. [CrossRef]
28. Langeheinecke, K.; Jany, P.; Thieleke, G.; Langeheinecke, K.; Kaufmann, A. *Thermodynamik für Ingenieure*; Springer Fachmedien Wiesbaden: Wiesbaden, Germany, 2013; ISBN 978-3-658-03168-8.
29. Chen, Z.; Zhang, Y.; Tang, W.; Lin, X.; Li, Q. Generic modelling and optimal day-ahead dispatch of micro-energy system considering the price-based integrated demand response. *Energy* **2019**, *176*, 171–183. [CrossRef]
30. 2004 IEEE International Conference on Robotics and Automation (IEEE Cat. No.04CH37508). In Proceedings of the 2004 IEEE International Conference on Robotics and Automation (IEEE Cat. No.04CH37508), New Orleans, LA, USA, 26 April–1 May 2004.
31. Gurobi Optimization. Gurobi Optimizer Reference Manual 2021. 2021. Available online: https://www.gurobi.com/documentation/9.5/refman/index.html (accessed on 6 December 2021).
32. Austrian Power Grid AG. Netzentwicklungsplan 2015: Für das Übertragungsnetz der Austrian Power Grid AG (APG), Wien, 2015. Available online: https://www.apg.at/~{}/media/009493CEFD824A85962F65CEAA6521C0.pdf (accessed on 18 November 2021).
33. Austrian Power Grid AG. Netzentwicklungsplan 2016: Für das Übertragungsnetz der Austrian Power Grid AG (APG), Wien, 2016. Available online: https://www.apg.at/~{}/media/2A8B8AC633414A359DB163BBE5104AD8.pdf (accessed on 18 November 2021).
34. Austrian Power Grid AG. Netzentwicklungsplan 2017: Für das Übertragungsnetz der Austrian Power Grid AG (APG), Wien, 2017. Available online: https://www.apg.at/~{}/media/6B16E721BF8D45F49A907C11A7C095EC.pdf (accessed on 18 November 2021).
35. Austrian Power Grid AG. Netzentwicklungsplan 2018: Für das Übertragungsnetz der Austrian Power Grid AG (APG), Wien, 2018. Available online: https://www.apg.at/-/media/B1CF20C3D97B4496AE3E06AF5B351AB7.pdf (accessed on 18 November 2021).
36. Austrian Power Grid AG. Netzentwicklungsplan 2019: Für das Übertragungsnetz der Austrian Power Grid AG (APG), Wien, 2019. Available online: https://www.apg.at/api/sitecore/projectmedia/download?id=bd6645e4-f83d-456a-a9d4-5757b5098a70 (accessed on 18 November 2021).
37. Austrian Power Grid AG. Netzentwicklungsplan 2020: Für das Übertragungsnetz der Austrian Power Grid AG (APG), Wien, 2020. Available online: https://www.apg.at/de/Stromnetz/Netzentwicklung#download (accessed on 18 November 2021).
38. Austrian Power Grid AG; LINZ NETZ GmbH; Netz Oberösterreich GmbH. Stromnetz-Masterplan Oberösterreich 2028: Ausbau des Hochspannungs-Stromnetzes (≥110 kV) in Oberösterreich. Planungszeitraum 2018–2028. 2018. Available online: https://www.land-oberoesterreich.gv.at/Mediendateien/Formulare/Dokumente%20UWD%20Abt_US/us-en_Stromnetz-Masterplan_Oberoesterreich_2028.pdf (accessed on 18 November 2021).
39. Land Kärnten. Energie Masterplan Kärnten, Klagenfurt. Available online: https://www.ktn.gv.at/DE/repos/files/ktn.gv.at/Abteilungen/Abt8/Dateien/energie/energiemasterplan%5fkaernten?exp=478252&fps=cbe8bb636710ede50d5a94df838d40cbaebea6d1 (accessed on 18 November 2021).
40. QGIS Development Team. QGIS Geographic Information System; Open Source Geospatial Foundation Project. 2021. Available online: http://qgis.osgeo.org (accessed on 18 November 2021).
41. Google. Map Data: Google, Terrametrics, Kartendaten (C) 2021. Available online: maps.google.at (accessed on 18 November 2021).
42. OpenStreetMap-Mitwirkende. OpenStreetMap. Available online: www.openstreetmap.org/copyright (accessed on 18 November 2021).
43. Austrian Power Grid AG. Statistische Netzdaten. Available online: https://www.apg.at/api/sitecore/projectmedia/download?id=703efbb9-bd69-49db-b2f6-bb676cac466b (accessed on 16 September 2020).
44. Heuck, K.; Dettmann, K.-D.; Schulz, D. (Eds.) *Elektrische Energieversorgung*; Springer Fachmedien Wiesbaden: Wiesbaden, Germany, 2013; ISBN 978-3-8348-1699-3.
45. Heuck, K.; Dettmann, K.-D.; Schulz, D. Anhang. In *Elektrische Energieversorgung*; Heuck, K., Dettmann, K.-D., Schulz, D., Eds.; Springer Fachmedien Wiesbaden: Wiesbaden, Germany, 2013; pp. 742–753.

46. AGGM Austrian Gas Grid Management AG. Unser Netz im Detail. Available online: https://www.gasconnect.at/netzinformationen/unser-netz-im-detail (accessed on 19 November 2021).
47. Austrian Gas Grid Management AGGM. *Erdgasinfrastruktur—Österreich: Georeferenzierte Darstellung nach Netzebenen*; Austrian Gas Grid Management AGGM: Wien, Austria, 2018.
48. Gas Connect Austria. *Erdgasleitungen & Erdgaslagerstätten in Österreich*; Gas Connect Austria: Wien, Austria, 2017.
49. E-Control. Erdgas—Bestandsstatistik: Leitungslängen zum 31. Dezember–Jahresreihen. Leitungslängen von Fern- und Verteilleitungen zum Jahresende. Available online: https://www.e-control.at/de/statistik/gas/bestandsstatistik (accessed on 19 November 2021).
50. Cerbe, G. *Grundlagen der Gastechnik: Gasbeschaffung, Gasverteilung, Gasverwendung*; Hanser: München, Germany, 2004; ISBN 978-3-446-22803-0.
51. Büchele, R.; Haas, R.; Hartner, M.; Hirner, R.; Hummel, M.; Kranzl, L.; Müller, A.; Ponweiser, K.; Bons, M.; Grave, K.; et al. Bewertung des Potentials für den Einsatz der hocheffizienten KWK und effizienter Fernwärme- und Fernkälteversorgung, Wien. 2015. Available online: https://ec.europa.eu/energy/sites/ener/files/documents/Austria_MNE%282016%2950514.pdf (accessed on 21 January 2021).
52. Bundesministerium Klimaschutz, Umwelt, Energie, Mobilität, Innovatoin und Technologie. Austrian Heat Map: Fernwärme und Kraft-Wärme-Kopplung in Österreich. Available online: http://www.austrian-heatmap.gv.at/das-projekt/ (accessed on 19 November 2021).
53. Navarro, A.; Rudnick, H. Large-Scale Distribution Planning—Part II: Macro-Optimization With Voronoi's Diagram and Tabu Search. IEEE Trans. *Power Syst.* **2009**, *24*, 752–758. [CrossRef]
54. Statistik Austria. STATatlas. Available online: https://www.statistik.at/atlas/ (accessed on 20 November 2021).
55. Statistik Austria. Nutzenergieanalyse. Available online: https://www.statistik.at/web_de/statistiken/energie_umwelt_innovation_mobilitaet/energie_und_umwelt/energie/nutzenergieanalyse/index.html (accessed on 20 November 2021).
56. Gobmaier, T.; Mauch, W.; Beer, M.; von Roon, S.; Schmid, T.; Mezger, T.; Habermann, J.; Hohlenburger, S. Simulationsgestütze Prognose des elektrischen Lastverhaltens, München. 2012. Available online: https://docplayer.org/5749688-Simulationsgestuetzte-prognose-des-elektrischen-lastverhaltens.html (accessed on 20 November 2021).
57. Austrian Power Clearing and Settlement. Synthetische Lastprofile: Prognose von Verbrauchswerten mittels Lastprofilen, Wien. 2019. Available online: https://www.apcs.at/de/clearing/technisches-clearing/lastprofile (accessed on 20 November 2021).
58. Dock, J.; Janz, D.; Weiss, J.; Marschnig, A.; Kienberger, T. Time- and component-resolved energy system model of an electric steel mill. *Clean. Eng. Technol.* **2021**, *4*, 100223. [CrossRef]
59. Groiss, C.; Grubinger, D.; Schwalbe, R. Blindleistungsbilanz im Salzburger Verteilnetz. In *EnInnov 2018: 15. Symphosium Energieinnovation*; Institut für Elektrizitätswirtschaft und Energieinnovation, Ed.; Verlag der Technischen Universität Graz: Graz, Austria, 2018; ISBN 978-3-85125-586-7.
60. Thormann, B.; Purgstaller, W.; Kienberger, T. Evaluating the potential of future e-mobility use cases for providing grid ancillary services. In Proceedings of the 26th International Conference and Exhibition on Electricity Distribution, Online, 20–23 September 2021.
61. BDEW; VKU; GEODE. BDEW/VKU/GEODE-Leitfaden: Abwicklung von Standardlastprofilen Gas, Berlin. 2016. Available online: https://www.bdew.de/media/documents/Leitfaden_20160630_Abwicklung-Standardlastprofile-Gas.pdf (accessed on 20 November 2021).
62. Pfenninger, S.; Staffell, I. Renewables.ninja. Available online: https://www.renewables.ninja/ (accessed on 20 November 2021).
63. Rienecker, M.M.; Suarez, M.J.; Gelaro, R.; Todling, R.; Bacmeister, J.; Liu, E.; Bosilovich, M.G.; Schubert, S.D.; Takacs, L.; Kim, G.-K.; et al. MERRA: NASA's Modern-Era Retrospective Analysis for Research and Applications. *J. Clim.* **2011**, *24*, 3624–3648. [CrossRef]
64. Oesterreichs Energie. Kraftwerkskarte Österreich. Available online: https://oesterreichsenergie.at/kraftwerkskarte-1 (accessed on 21 November 2021).
65. Oesterreichs Energie. *Stromerzeugung in Österreich: Kraftwerke der Österreichischen E-Wirtschaft*; Oesterreichs Energie: Vienna, Austria, 2019.
66. Crastan, V. *Elektrische Energieversorgung 2*; Springer: Berlin/Heidelberg, Germany, 2008; ISBN 978-3-540-70877-3.
67. Verbund. Unsere Kraftwerke. Available online: https://www.verbund.com/de-at/ueber-verbund/kraftwerke/unsere-kraftwerke (accessed on 21 November 2021).
68. Wikipedia. Liste von Wasserkraftwerken in Österreich. Available online: https://de.wikipedia.org/wiki/Liste_von_Wasserkraftwerken_in_%C3%96sterreich (accessed on 21 November 2021).
69. KELAG AG. Kraftwerke. Available online: https://www.kelag.at/kraftwerke (accessed on 21 November 2021).
70. TIWAG. Kraftwerkspark: Unsere Kraftwerke im Überblick. Available online: https://www.tiwag.at/ueber-die-tiwag/kraftwerke/bestehende-kraftwerke/kraftwerkspark/ (accessed on 21 November 2021).
71. Energie AG. Die Wasserkraftwerke der Energie AG Oberösterreich. Available online: https://www.energieag.at/Themen/Energie-fuer-Sie/Kraftwerke/Wasserkraftwerke (accessed on 21 November 2021).
72. Salzburg AG. Unsere Erzeugungsanlagen. Available online: https://www.salzburg-ag.at/ueber-die-salzburg-ag/unternehmen/erzeugung/erzeugungsanlagen.html (accessed on 21 November 2021).

73. VERBUND Hydro Power AG. *Strom aus den Hohen Tauern: Die Wasserkraftwerke in Salzburg*; VERBUND Hydro Power AG: Vienna, Austria, 2013.
74. VERBUND Hydro Power AG. *Strom aus den Zillertaler Alpen: Die Wasserkraftwerke in Tirol*; VERBUND Hydro Power AG: Vienna, Austria, 2013.
75. VERBUND Hydro Power AG. *Strom aus den Hohen Tauern und aus der Drau: Die Wasserkraftwerke in Kärnten*; VERBUND Hydro Power AG: Vienna, Austria, 2013.
76. Illwerke VKW. Kraftwerksanlagen der Illwerke VKW. Available online: https://www.illwerkevkw.at/kraftwerke_uebersicht.htm (accessed on 21 November 2021).
77. Energie Steiermark. Wasserkraft. Available online: https://www.e-steiermark.com/ueber-uns/energieerzeugung/wasserkraft (accessed on 21 November 2021).
78. EVN Naturkraft. Wasserkraft. Available online: http://www.evn-naturkraft.at/Oekostrom/Wasser.aspx (accessed on 21 November 2021).
79. Geodatenstellen des Landes Tirol. *TIRIS*; Amt der Tiroler Landesregierung: Innsbruck, Austria; Available online: https://maps.tirol.gv.at (accessed on 22 November 2021).
80. Bundesministerium für Landwirtschaft, Regionen und Tourismus. eHYD. Available online: https://ehyd.gv.at/ (accessed on 16 November 2021).
81. Kleinwasserkraft Österreich. Nutzen der Kleinwasserkraft. Available online: https://www.kleinwasserkraft.at/en/fakten/ (accessed on 21 November 2021).
82. Pöyry. Wasserkraftpotenzialstudie Österreich. 2018. Available online: https://oesterreichsenergie.at/fileadmin/user_upload/Oesterreichs_Energie/Publikationsdatenbank/Studien/2018/WasserkraftpotenzialOesterreich2018.pdf (accessed on 21 November 2021).
83. TIWAG. *Kraftwerksgruppe Sellrain-Silz*; Kraftwerksgruppe Sellrain-Silz. TIWAG: Innsbruck, Austria; Available online: https://www.tiwag.at/unternehmen/unsere-kraftwerke/kraftwerk/kraftwerksgruppe-sellrain-silz/ (accessed on 21 November 2021).
84. KELAG AG. Pumpspeicherkraftwerke. Available online: https://www.kelag.at/corporate/pumpspeicherkraftwerke-852.htm (accessed on 21 November 2021).
85. TIWAG. Unsere Kraftwerksprojekte. Available online: https://www.tiwag.at/ueber-die-tiwag/kraftwerke/wasserkraftausbau/unsere-kraftwerksprojekte/ (accessed on 21 November 2021).
86. Verbund. Pumpspeicherkraftwerk Limberg 3. Available online: https://www.verbund.com/de-at/ueber-verbund/kraftwerke/unsere-kraftwerke/kaprun-oberstufe-limberg-3 (accessed on 21 November 2021).
87. Zahoransky, R. *Energietechnik*; Springer: Wiesbaden, Germany, 2019; ISBN 978-3-658-21846-1.
88. Österreichischer Biomasse-Verband. *Bioenergie Atlas Österreich 2019*, 2nd ed.; Österreichischer Biomasse-Verband: Wien, Austria, 2019; ISBN 978-3-9504380-3-1.
89. ÖVGW. Montanuniversität Leoben, WU Wien, DBI Gas- und Umwelttechnik GmbH, TU Wien, JKU Linz, ERIG. Greening the Gas: Forschungsbericht 2019, Vienna. 2020. Available online: https://www.ovgw.at/media/medialibrary/2020/03/OVGW_JB_forschung19_hi_corr2.pdf (accessed on 21 November 2021).
90. Photovoltaik Austria. Die österreichische Photovoltaik & Speicher-Branche in Zahlen, Wien. 2020. Available online: https://www.pvaustria.at/wp-content/uploads/2020_07_05_Fact_Sheet_PV_Branche.pdf (accessed on 22 November 2021).
91. Pfenninger, S.; Staffell, I. Long-term patterns of European PV output using 30 years of validated hourly reanalysis and satellite data. *Energy* **2016**, *114*, 1251–1265. [CrossRef]
92. The Wind Power. Windparks—Österreich. Available online: https://www.thewindpower.net/windfarms_list_de.php?country=AT (accessed on 10 December 2020).
93. Staffell, I.; Pfenninger, S. Using bias-corrected reanalysis to simulate current and future wind power output. *Energy* **2016**, *114*, 1224–1239. [CrossRef]
94. LINZ AG. Die Kraftwerke der LINZ AG: Effiziente, umweltschonende Energieerzeugung, Linz. 2018. Available online: https://www.linzag.at//media/dokumente/linzag/folder-kraftwerke.pdf (accessed on 22 November 2021).
95. EVN. Thermische Erzeugung. Available online: https://www.evn.at/EVN-Group/Energie-Zukunft/Energie-aus-Niederosterreich/Gas-und-Kohle.aspx (accessed on 22 November 2021).
96. Wien Energie. Energie ist unsere Verantwortung: Konsolidierte Umwelterklärung 2021 der Strom- und Wärmeerzeugungsanlagen der Wien Energie GmbH gemäß EMAS-Verordnung, Wien. 2021. Available online: https://dokumente.wienenergie.at/wp-content/uploads/umwelterklaerung-2021.pdf (accessed on 22 November 2021).
97. Energie AG. Übersicht thermische Kraftwerke. Available online: https://www.energieag.at/Themen/Energie-fuer-Sie/Kraftwerke/Thermische-Kraftwerke (accessed on 22 November 2021).
98. ENTSO-E. Transparancy Platform. Available online: https://transparency.entsoe.eu (accessed on 22 November 2021).
99. Krutzler, T.; Zechmeister, A.; Stranner, G.; Wiesenberger, H.; Gallauner, T.; Gössl, M.; Heller, C.; Heinfellner, H.; Ibesich, N.; Lichtblau, G.; et al. *Energie- und Treibhausgas-Szenarien im Hinblick auf 2030 und 2050: Synthesebericht 2017*; Umweltbundesamt: Wien, Austria, 2017; ISBN 978-3-99004-445-2.
100. Österreich.gv.at. Sanierungsoffensive 2021/2022. Available online: https://www.oesterreich.gv.at/themen/bauen_wohnen_und_umwelt/energie_sparen/1/sanierungsoffensive.html (accessed on 23 November 2021).

101. Statistik Austria. Kraftfahrzeuge—Bestand. Available online: https://www.statistik.at/web_de/statistiken/energie_umwelt_innovation_mobilitaet/verkehr/strasse/kraftfahrzeuge_-_bestand/index.html (accessed on 23 November 2021).
102. ÖAMTC; ARBÖ. Expertenbericht Mobilität & Klimaschutz 2030, Wien. 2018. Available online: https://www.oeamtc.at/%C3%96AMTC+Expertenbericht+Mobilit%C3%A4t+%26+Klimaschutz+2030+Web.pdf/25.789.593 (accessed on 23 November 2021).
103. Umweltbundesamt. Verkehrsmittel in Österreich. Available online: https://www.umweltbundesamt.at/fileadmin/site/themen/mobilitaet/daten/ekz_doku_verkehrsmittel.pdf (accessed on 23 November 2021).
104. ADAC. Elektroautos im Test: So hoch ist der Stromverbrauch. Available online: https://www.adac.de/rund-ums-fahrzeug/tests/elektromobilitaet/stromverbrauch-elektroautos-adac-test/ (accessed on 23 November 2021).
105. Hartl, M.; Biermayr, P.; Schneeberger, A.; Schöfmann, P. Österreichische Technologie-Roadmap für Wärmepumpen, Wien. 2016. Available online: https://nachhaltigwirtschaften.at/resources/nw_pdf/1608_endbericht_oesterreichische_technologieroadmap_fuer_waermepumpen.pdf?m=1469661515& (accessed on 23 November 2021).
106. Weniger, J.; Orth, N.; Lawaczeck, I.; Meissner, L.; Quaschning, V. Energy Storage Inspection 2021, Berlin, 2021. Available online: https://pvspeicher.htw-berlin.de/wp-content/uploads/Energy-Storage-Inspection-2021.pdf (accessed on 23 November 2021).
107. Statistik Austria. Energiebilanzen. Available online: http://www.statistik.at/web_de/statistiken/energie_umwelt_innovation_mobilitaet/energie_und_umwelt/energie/energiebilanzen/index.html (accessed on 20 November 2021).
108. Thormann, B.; Kienberger, T. Evaluation of Grid Capacities for Integrating Future E-Mobility and Heat Pumps into Low-Voltage Grids. *Energies* **2020**, *13*, 5083. [CrossRef]
109. Thormann, B.; Kienberger, T. Estimation of Grid Reinforcement Costs Triggered by Future Grid Customers: Influence of the Quantification Method (Scaling vs. Large-Scale Simulation) and Coincidence Factors (Single vs. Multiple Application). *Energies* **2022**, *15*, 1383. [CrossRef]
110. Shi, H.; Blaauwbroek, N.; Nguyen, P.H.; Kamphuis, R. Energy management in Multi-Commodity Smart Energy Systems with a greedy approach. *Appl. Energy* **2016**, *167*, 385–396. [CrossRef]
111. Xie, Y.; Ueda, Y.; Sugiyama, M. Greedy energy management strategy and sizing method for a stand-alone microgrid with hydrogen storage. *J. Energy Storage* **2021**, *44*, 103406. [CrossRef]
112. Energy Exchange Austria. Historische Marktdaten. Available online: https://www.exaa.at/marktdaten/historische-marktdaten/ (accessed on 15 January 2020).
113. Kays, J.; Seack, A.; Smirek, T.; Westkamp, F.; Rehtanz, C. The Generation of Distribution Grid Models on the Basis of Public Available Data. *IEEE Trans. Power Syst.* **2017**, *32*, 2346–2353. [CrossRef]
114. Esslinger, P.; Witzmann, R. Entwicklung und verifikation eines stochastischen Verbraucherlastmodells für Haushalte. In *12. Symposium Energieinnovation: Alternativen für die Energiezukunft Europas*; Elektrizitatswirtschaft und Energieinnovation, Ed.; Verlag der Technischen Universitat Graz: Graz, Austria, 2012; ISBN 978-3-85125-200-2.
115. Ringkjøb, H.-K.; Haugan, P.M.; Solbrekke, I.M. A review of modelling tools for energy and electricity systems with large shares of variable renewables. *Renew. Sustain. Energy Rev.* **2018**, *96*, 440–459. [CrossRef]